GENE PROFILING IDENTIFIES COMMONALITIES IN NEURONAL PATHWAYS IN EXCITOTOXICITY: EVIDENCE FOR CELL CYCLE RE-ACTIVATION IN CONCERT WITH OXIDATIVE STRESS

Minghui Jessica Chen[¶1], Jian Ming Jeremy Ng[¶1], Zhao Feng Peng[2,3], Jayapal Manikandan[4], Yann Wan Yap[6], Roxana M. Llanos[6], Philip M. Beart*[5], Nam Sang Cheung*[6]

[1]Menzies Research Institute, University of Tasmania, Hobart, Tasmania 7000, Australia.

Department of [2]Biochemistry, Yong Loo Lin School of Medicine, National University of Singapore, 8 Medical Drive, Singapore 117597.

[3]Key Laboratory of Biogeology and Environmental Geology of the Ministry of Education, University of Geosciences, Wuhan 430074, P.R. China

[4]Center of Excellence in Genomic Medicine Research (CEGMR), King Fahad Medical Research Center, King AbdulAziz University, Jeddah 21589, Saudi Arabia

[5]Florey Neuroscience Institutes and Department of Pharmacology, University of Melbourne, Victoria 3010, Australia

[6]Centre for Cellular and Molecular Biology, School of Life and Environmental Sciences, Deakin University, Burwood, Victoria 3125, Australia.

[¶] Minghui Jessica Chen and Jian Ming Jeremy Ng contributed equally to this study.

* Joint-corresponding authors and to whom proofs and reprint requests should be addressed: Dr Steve Nam Sang Cheung, School of Life and Environmental Sciences, Deakin University, Burwood, Victoria 3125, Australia. Tel: +613 92446100, E-mail: steve.cheung@deakin.edu.au

Running title: Commonalities in iGluRs global gene profiles

Abstract:

Excitotoxicity, induced by the aberrant rise in cytosolic Ca^{2+} level, is a major neuropathological process in numerous neurodegenerative disorders. It is triggered when extracellular glutamate (Glu) concentration reaches neuropathological levels resulting in dysregulation and hyper-activation of ionotropic glutamate receptor subtype (iGluRs). Even though all three members of the iGluRs, namely N-methyl-D-aspartate (NMDAR), α-amino-3-hydroxy-5-methyl-4-isoxazolepropionic acid (AMPAR) and kainate (KAR) receptors are implicated in excitotoxicity, their individual contributions to downstream signaling transduction have not been explored. In this study, we report a comprehensive description of the recruitment of cellular processes in neurons upon iGluR activation during excitotoxicity through temporal (5h, 15h and 24h) global gene profiling of AMPA, KA, NMDA and Glu excitotoxic models. DNA microarray analyses of mouse primary cortical neurons treated with these four pharmacological agonists are further validated via real-time PCR. Bi-model analyses against Glu model demonstrate that NMDARs and KARs play a more pivotal role in Glu-mediated excitotoxicity, with a higher degree of global gene profiling overlaps, as compared to that of AMPARs. Comparison of global transcriptomic profiles reveals aberrant calcium ion binding and homeostasis, organellar (lysosomal and endoplasmic reticulum) stress, oxidative stress, cell cycle re-entry and activation of cell death processes as the main pathways that are significantly modulated across all excitotoxicity models. Singular profile analyses demonstrate substantial transcriptional regulation of numerous cell cycle proteins. For the first time, we show that iGluR activation forms the basis of cell cycle re-activation, and together with oxidative stress fulfill the "two-hit" hypothesis that accelerates neurodegeneration.

(246 words)

Keywords

- Excitotoxicity
- ionotropic
- Glutamate
- Ischemic stroke
- Cell cycle re-activation
- Neuronal death
- Microarray

Number of tables: 3

Number of figures: 4

Number of supplementary tables: 4

1. Contract Grant sponsor: NHMRC Project Grant APP1023646
2. PMB is a Research Fellow (APP1020401) of the NHMRC (Australia).

1. Introduction

Excitotoxicity is a general term that defines a damage-inflicting cellular process mediated via overstimulation of receptors for L-glutamate (GluRs) to effect a rise in cytosolic calcium ion level and occurs principally as a result of a constitutive and hyper-activation of ion channel-gated GluRs (iGluRs) and other types of calcium channels (Arundine and Tymianski, 2003). Because cellular indices reflecting excitotoxic damage are altered early in the pathogenesis of various neurodegenerative diseases such as Alzheimer's disease (AD; (Hynd et al., 2004)), dementia associated with Down syndrome (DS; (Scheuer et al., 1996)) and acute neurological deficits due to traumatic brain injury (TBI) and stroke (Arundine and Tymianski, 2004), excitotoxicity is believed to be one of the primary upstream events that induces neuronal injury at a cellular level. An extracellular rise in the concentration of L-glutamate (Glu) in the micro-environment of the brain is recognized as a key trigger for initiating excitotoxicity and has been documented in conditions such as hypoglycemia or status epilepticus (Costa et al., 2004; Ding et al., 2007; Wieloch et al., 1985). Hypoglycemia is commonly observed during both stroke and an episode of TBI where ischemic reduction in blood flow limits supply of oxygen and glucose to a localized region of the brain. These events then lead to inadequate ATP production which abolishes the electrochemical gradients required to maintain functionality of inward-rectifying Glu transporters in astrocytes, resulting in an accumulation of extracellular Glu. To further complicate matters, the loss of electrochemical gradients reverses the channeling action of these transporters, causing them to release Glu into the extracellular space. This reversal has important neuronal implications as it further enhances the accumulation of extracellular Glu, which then causes a potentiation of dysregulated GluRs in neighboring neurons, leading to intracellular calcium imbalance and subsequently and their demise (Beart and O'Shea , 2007).

Basically, Glu is the only physiological excitatory neurotransmitter agonist for GluR activation in the mammalian brain. Because GluRs activation is a major determinant of synaptic plasticity, it plays an important role in structuring neurocognitive processes underlying memory and learning (Mukherjee and Manahan-Vaughan, 2012). The subunit composition and sequence homology of each GluR in its superfamily have been extensively studied and depending on their individual mode of activation, they are grouped into either metabotropic (mGluRs) or ionotropic (iGluRs) GluRs (Niciu et al., 2012). While mGluRs indirectly activate ion channel via signaling pathways that involve G proteins, iGluRs possess intrinsic ion channel activities. Therefore, during excitotoxicity, neuronal cell death is mediated by two concurrent yet distinct signaling processes determined by both iGluRs and mGluRs (Lea and Faden, 2003).

In particular, iGluRs are made up of N-methyl-D-aspartate (NMDA), α-amino-3-hydroxy-5-methyl-4-isoxazolepropionic acid (AMPA) and kainate (KA) receptor subtypes which are named after their specific pharmacological agonists active at different intrinsic ligand-gated ion channel activity that allows passage of Na^+ and Ca^{2+} ions through a pore. All three subtypes of iGluRs (NMDAR, AMPAR and KAR) are actively involved during excitotoxic neuronal cell death. The NMDAR plays a major role due to its abundant expression and highest Ca^{2+} permeability (Hara and Snyder, 2007). Studies have shown that excessive NMDAR activation induces Ca^{2+} influx and release from intracellular stores, resulting in the activation of cytoplasmic proteases such as calcium-activated calpains (Simpkins et al., 2003) that hydrolyze cytoskeletal proteins. An example of such cytoskeletal protein is α-fodrin (Posner et al., 1995; Siman et al., 1989). Furthermore, NMDAR activation can result in the destabilization of lysosomes and the release of lysosomal cathepsins, causing cell death

(Graber et al., 2004; Tenneti et al., 1998). Likewise, dysregulation of AMPAR and KAR also induces excitotoxicity in neurons (Jayakar and Dikshit, 2004; Sattler and Tymianski, 2001; Vincent and Mulle, 2009). Indeed, we were the first to demonstrate that AMPA alone could produce apoptotic-like injury (Larm et al., 1997), just as can KA, with injury likely to exert an apoptotic-necrotic continuum of programmed cell death (Cheung et al., 1998).

To date, the consequences of activation of individual iGluRs subtypes in downstream signal transduction during excitotoxicity has not been comprehensively and simultaneously explored in a comparative platform, impeding an understanding of the relative contributions of individual iGluRs, be that via convergent or divergent cellular pathways, towards excitotoxic damage. In our current study, global transcriptomic profiling was employed to elucidate downstream signaling pathways, in terms of amplification and diversification, subsequent to different iGluR activation to model the sequence of events subsequent to extracellular Glu in the brain reaching pathological concentrations. Here, the DNA microarray technique was applied to four excitotoxic models induced by a) the general GluR agonist, Glu, b) AMPAR agonist, AMPA, c) NMDAR agonist, NMDA and d) KAR agonist, KA. Subsequent comparative global gene profile analysis was performed to elucidate the major primary biological processes regulated by iGluRs in the trigger of excitotoxicity during Glu-mediated neuronal injury. Our study is the first to attempt global gene profiling of this type and scale to elucidate the pathobiology of excitotoxicity. Briefly, oxidative stress and cell cycle re-activation were identified as the primary cellular pathways that were significantly modulated. The specific association of cell cycle-reactivation with iGluR activation provided interesting evidence for the occurrence of a ‘two-hit’ hypothesis in excitotoxicity that has been previously postulated by others for the basis of neurodegeneration in AD pathogenesis (Zhu et al., 2004, 2007).

2. Materials and methods

2.1 Murine Neocortical Neuronal Cultures

Neocortical neurons (gestational days 15 or 16) obtained from foetal cortices of Swiss albino mice were used to prepare the primary cultures as previous described with minor modifications (Cheung et al., 2000). Dissected cortices were subjected to trypsin digestion and mechanical trituration. Cells were collected by centrifugation and resuspended in Neurobasal™ (NB) medium containing 2.5% B27 supplement, 1% penicillin, 1% streptomycin, 0.25% GlutaMAX-1 supplement and 10% dialyzed foetal calf serum. 24-Well plates previously coated with poly-D-lysine (100μg/ml) were seeded with cells to a density of 2×10^5 cells/cm^2 and used for subsequent experiments. Cultures were maintained in a humidified 5% CO_2 and 95% air incubator at 37°C. Immunocytochemical staining of the cultures at day 5 *in vitro* for microtubule-associated protein-2 and glial fibrillary acidic protein revealed > 95% of the cells were neurons with minimal contamination by glia (Cheung et al., 1998). All experiments involving animals were approved by the National University of Singapore, and were in accordance with the US Public Health Service guide for the care and use of laboratory animals.

2.2 Drug Preparation and Treatment

Glu, NMDA, KA and *S*-AMPA (Sigma-Aldrich) were freshly prepared prior to usage to achieve stock concentrations of 100mM. Working concentrations (Glu 250 μM, NMDA 200 μM, KA 100 μM and *S*-AMPA 300 μM) were achieved by dilution with NB medium.

2.3 Total RNA extraction and isolation

RNA was extracted using RNeasy Mini Kit (Qiagen Cat. No. 74104) according to the manufacturer's instructions. All pipette tips used were RNase-free. Each sample was prepared from 1×10^6 cultured cells. RNA concentration was determined spectrophotometrically using Nanodrop ND-1000 Version 3.2.1 and RNA quality was determined using a E-gene HDA-GT12 genetic analyzer.

2.4 Microarray analysis using Illumina Mouse Ref8 Ver.1.1 hybridization beadchips

Microarray was carried out using Illumina® Mouse Ref8 Ver.1.1 arrays. For each GluR agonist treatment, the assignment of the arrays was as follow: 5h (n=3), 15h (n=3), and 24h (n=3) and control (n=6). Each RNA sample (500ng) was reverse transcribed using T7 Oligo(dT) primer to form first strand cDNA containing a T7 promoter sequence, which was subsequently used for the second strand cDNA synthesis (employing DNA polymerase and Rnase H to simultaneously degrade the RNA and to synthesize second strand cDNA). The cDNAs were purified to remove RNA, primers, enzymes, and salts that would inhibit *in vitro* transcription. Finally *in vitro* transcription was employed to generate multiple copies of biotinylated cRNA from the double-stranded cDNA templates. All previously mentioned procedures were performed using Illumina® TotalPrep RNA Amplification Kit. cRNA yields were quantitated using the NanoDrop ND-1000.

cRNA (750ng) prepared in RNase-free water (5μl) was mixed with hybridization buffer (10μl) and preheated to 65°C for 5min. Assay samples were then fully loaded onto the large sample port of each array on the beadchip. Beadchips were incubated in a humidified hybridization chamber at 58°C for

17h. The following day, the IntelliHyb seal on the beadchip was removed to expose all the arrays. Beadchips were blocked and labeled with streptavidin-Cy3, followed by stringency buffer washes and dried. The hybridization process was carried out according to the manufacturer's instruction (Illumina Inc.). Beadchips were then ready for scanning on the Illumina® scanner using Bead Studio software at Scan Factor = 0.8.

2.5 Microarray data collection and analysis

Initial analysis of the scanned images was performed using BeadScan (Illumina). The absolute data (signal intensity, detection call and detection P-value) were exported into GeneSpringGX 7.3 (Agilent Technologies, CA, USA) software for analysis by a parametric test based on crossgene error model (PCGEM). A one-way analysis of variance (ANOVA) approach was used to identify differentially expressed genes. Array data were globally normalized using GeneSpring software. Firstly, all measurements on each chip were divided by the 50^{th} percentile value (per chip normalization). Secondly, each gene was normalized to the baseline value of the control samples (per gene normalization) using median. Then genes were filtered on fold change ±1.5 fold against controls in at least one of three conditions for each respective treatment. Finally, one-way ANOVA ($p < 0.05$) and Benjamini-Hochberg False Discovery Rate (FDR) Correction were used to seek differentially expressed genes. Genes which were differentially expressed are annotated according to Gene Ontology-Biological process provided by the online bioinformatics resources Database for Annotation, Visualization and Integrated Discovery (DAVID) 6.7 (http://david.abcc.ncifcrf.gov/) (Dennis et al., 2003; Huang et al., 2009). All microarray data reported here are described in accordance with MIAME guidelines, and has been deposited in the NCBIs Gene Expression

Omnibus (GEO; http://www.ncbi.nlm.nih.gov/geo/) and are accessible through GEO Series accession number GSE16035, GSE22993, GSE22994 and GSE19936.

2.6 Real-time polymerase chain reaction (PCR)

Eight differentially expressed genes were selected for validation of the microarray results in replicate by quantitative real-time PCR in three independent experiments. The same total RNAs used for microarray from mouse culture treated with 250 μM Glu were reverse transcribed to cDNAs according to steps specified by the manufacturer (Applied Biosystems Taqman reverse transcription reagents). The experiment set up, briefly, consisted of Taqman master mix (20μl) and cDNA or water (NTC; both 5μl) was added to the designated reaction well of a real-time PCR plate. The plate was then read using the 7000 Fast Real-Time PCR System with conditions according to the manufacturer's protocol.

3. Results

Overall, cellular transcriptional regulation was assessed in excitotoxic models employing 250 μM Glu, 200 μM NMDA, 300 μM AMPA and 100 μM KA over a 24-hour period using Illumina® Mouse Ref8 V1.1 genechips. The raw transcriptional signal data from individual arrays were then subjected to statistical filtering using one-way ANOVA, $p < 0.05$ and Benjamini-Hochberg FDR. Gene probes were considered to be significantly regulated when they demonstrated gene expression changes of at least ± 1.5 folds in a minimum of one out of the three time-points (5h, 15h and 24h). All gene probes that passed these selection criteria were gathered to form the global transcriptomic data for each excitotoxic model. Transcriptomic profiles generated from the treatment of neurons with Glu (1,842 gene probes), NMDA (2,309 gene probes), AMPA (1,563 gene probes) and KA (3,800 gene probes) were organized side-by-side and partitioned to different fold-change categories (Figure 1). A substantial number of gene probes demonstrated greater than ±1.5 fold-changes in gene expression over the 24-hour period, with KA treatment generating the largest transcriptomic profile.

3.1 Bi-model analyses of individual iGluRs profiles against that of Glu revealed the following decrease ordering of iGluRs activation dependence NMDARs>KARs>AMPARs during excitotoxicity

Bi-model global transcriptomic profile comparisons using Glu model as the basis of analysis demonstrated that in rank order of highest to lowest degree of overlap, i.e. commonly occurring and differentially regulated gene probes, NMDA > KA > AMPA (Figure 2). NMDA (Figure 2A) and KA (Figure 2C) profiles were comparable, but they exhibited nearly double the number of Glu commonly

occurring genes when compared to AMPA profile (Figure 2B). These profiles signify a greater reliance upon NMDAR and KAR-mediated signaling pathways to induce excitotoxicity during Glu-mediated neurotoxicity. A more in-depth analysis of the consistency in transcriptional regulatory trend demonstrated that the majority of the genes were similarly regulated at 15h and 24h respectively in all three iGluRs models (Figure 3).

3.2 Simultaneous comparison of all four excitotoxic models identified several major common biological processes

A concerted transcriptomic analysis of all four profiles revealed a total list of 583 common genes. Similarly, a detailed exploration of the transcriptional trend of these genes revealed a high degree of consistency at each respective time-point, which faltered upon inter-time-point examination across all three time-points (Figure 4), indicating a common temporal activation and/or inhibition of signaling pathways across all four excitotoxicity models, but with distinct progression outcome of each signaling cascade, i.e. either pursuant and persistent maintenance of initial activated/inhibitory state or directional change of pathway regulation.

Functional classification of these 583 RefSeq transcripts, which corresponded to 485 biologically-annotated genes, identified several important and over-represented biological pathways relevant to the progression of excitotoxicity (Table 1). These include calcium homeostasis and binding, anti-oxidant response, cell death and cell survival processes. Notably, an overwhelming number of molecules involved in the promotion of mitotic cell cycle progression were transcriptionally elevated in all four models of excitotoxicity. Consistently, all members of these over-represented biological

processes were significantly modulated at the expression level between the 5h and 15h time-points, implying the reported pathways constitute the early upstream cellular events in excitotoxicity.

I. **Calcium ion homeostasis and binding:** In all four excitotoxic models, genes encoding for Ca^{2+}-dependent proteins and receptors (Gpr12, Prkcb and Rxfp3) were significantly down-regulated, indicating the occurrence of aberrant calcium ion homeostasis. On the contrary, genes encoding for Ca^{2+}-binding proteins (S100a6 and Anx (A2, A3 and A5) showed increased gene expression, providing further evidence of elevation of cytosolic Ca^{2+}level during excitotoxicity due to activation of iGluRs which triggers intrinsic Ca^{2+}channel activity.

II. **Lysosomal stress:** Aberrant elevation of cytosolic Ca^{2+} ion level and overproduction of reactive oxygen species (ROS) imposes organellar stress through disruption of the delicate balance of cellular ionic gradients and unregulated modifications of cellular proteins resulting in detrimental loss/gain-of function, all contributing to disturbance of normal cellular signaling. Analysis of the gene profiles of genes common to all four excitotoxic models revealed significant transcriptional activation of lysosomal resident proteins, indicative of some form of disorientation and/or stress imposed on the normal functioning of the lysosomes.

III. **Anti-oxidant responses**

Heat shock proteins (Hsps) and molecular chaperones: Organellar (ER and lysosomal) stress is especially prominent in excitotoxicity and evokes a cellular counteractive response to minimize electrophilic and oxidative burdens. Interestingly, comparative microarray analysis

demonstrated that in our specific iGluR excitotoxic models, up-regulation of the majority of genes encoding for heat shock proteins (HSPs) and molecular chaperones (Hmox1, Srxn1, Hspa2, and Hspb8) and metal chaperones (Mt3) occurred at the 5h time-point, much earlier than that of Glu at 15h.

Glutathione (GSH) metabolism: Genes transcribing for members of the GSH anti-oxidative pathway were significantly up-regulated in all four models. However, AMPA and Glu models demonstrated significant elevation of GSH pathway genes at 15h, while NMDARs and KARs demonstrated earlier transcriptional response at 5h.

IV. **Cell death:** Majority of the genes encoding for proteins directly/indirectly involved in promotion of cell death (Angptl4, Casp6 and Ctnna1) were transcriptionally up-regulated. In addition, cell death was further accelerated by the down-regulation of anti-cell death protein (Bcl11b).

V. **Cell homeostasis, survival and proliferation:** In all four excitotoxic models, genes encoding for pro-survival/mitogenic proteins (Spp1 and Birc5 (also known as Survivin)) and growth factors (Igf2 and Igfbp5) were up-regulated between the 5h and 15h time-points. These responses indicate a cellular response to suppress cell death mechanisms.

VI. **Mitotic cell cycle:** Numerous genes encoding for cell cycle proteins that promote cell cycle re-entry were up-regulated in all four excitotoxic models between 5h and 15h. This observation is totally unprecedented in the context of excitotoxicity. Under physiological

conditions, neurons are in the post-mitotic and differentiated state. Aberrant cell cycle re-entry has been implicated in the pathogenesis of several neurological conditions such as AD, DS, Huntington's disease, Pick's disease and stroke (Camins et al., 2008; Pelegri et al., 2008). Recent studies on AD suggested this cellular event to be a part of the neuronal death process (Lopes et al., 2009a, 2009b). p53, the main keeper of genome integrity, was significantly down-regulated (denoted as Trp53 in the table), indicating a failure in the cell cycle checkpoint system that enhances re-activation of cell cycle process.

3.3 Singular profile analysis highlights cell cycle re-activation as a prominent biological process during excitotoxicity

The majority of proteins involved in mitotic cell cycle process showed significant transcriptional modulation across all four profiles (Table 2). Gene expression of proteins promoting positive regulation of mitosis occurred between 5h and 15h post-treatment, providing strong evidence for the early occurrence of cell cycle re-entry upon iGluRs induction. Detailed temporal fold-expression of individual genes can be found in Supplementary Tables 1-4.

3.4 Validation of Glu global transcriptomic profiles via real-time PCR

Microarray data were validated via real-time PCR using the same total RNA samples previously employed for microarray analysis. Similar temporal transcriptional regulatory trends were observed for the genes listed in Table 3.

4. Discussion

Excitotoxicity is well accepted to be a cell death process contributing to both acute and chronic neurodegenerative conditions (Doble, 1999). Although rises in intracellular Ca^{2+} subsequent to activation of NMDARs play a central role in most discussions of excitotoxicity, the recruitment of cell signaling cascades is likely to be more complex. Here, we sought to determine the individual contributions of over-stimulated iGluRs to the excitotoxic process by transcriptomic profiling. The rationale here was that gene expression profiling using the robust approach of primary cultured neurons with well controlled experimental conditions would allow a thorough understanding of which molecules are involved downstream of individual iGluR activation and then contribute towards the excitotoxic process of neuronal cell death. Previously, we have demonstrated the expression of functional iGluRs in our neuronal culture model (Cheung et al., 2007). Key findings obtained by comparison of global transcriptomic profiles were that the main pathways modulated across all excitotoxic models were calcium ion binding and homeostasis, organellar stress, oxidative stress, cell cycle re-activation and activation of cell death processes. Notably, we show for the first time that iGluR activation forms the basis of cell cycle re-activation, and that with oxidative stress they together fulfill the "two-hit" hypothesis that accelerates neurodegeneration.

Simultaneous comparison of the global transcriptomic profiles of AMPA-, KA-, NMDA- and Glu-mediated excitotoxic injury revealed a higher degree of correlation in terms of number of similarly-regulated genes for KA and NMDA, rather than AMPA profiles, versus that of Glu as background. Importantly, these data suggest that as compared to AMPARs, a higher amplification of signalling transduction from KARs and NMDARs activation may be due to their greater expression on cell

surfaces, which often have a direct graded influence on intrinsic receptor ionic conductance and/or recruiment of elicited downstream pathways. Other than not being as highly expressed as NMDARs, AMPARs are depolarized before NMDARs and they demonstrate differential Ca^{2+} permeability which is governed by the presence or absence of the GluR2 subunit (Bassani et al., 2009; Wright and Vissel, 2012). As such, the presence or absence of GluR2 plays a crucial role in AMPAR-mediated Ca^{2+} influx in neurons under Glu stimulus. Based on these reported physiological differences, a different transcriptomic profile might be expected. In the case of Glu, delay in cellular process activation may be accounted by dilution of the effective concentration of the agonist to activate iGluRs, due to concurrent sequestration of Glu molecules by mGluRs and Glu transporters.

Functional annotation revealed oxidative stress and cell cycle re-activation as the main cellular components triggered by excitotoxicity. Presence of oxidative stress is likely a response to the transcriptional upregulation of organellar (ER/lysosomal) stress-inducible genes and anti-oxidant proteins such as Hsps, molecular chaperones and GSH enzymes. More interesting was that the origin of cell cycle-reactivation has been defined for the first time and clearly linked to iGluR activation. Overall, simultaneous transcriptional upheaval of both processes supports the “two-hit” hypothesis originally formulated for AD pathogenesis (Zhu et al., 2001, 2004, 2007), suggesting that oxidative stress and cell cycle dysregulation contribute hand-in-hand to neuronal loss during neurodegeneration.

Temporal global transcriptomic profiles of models of excitotoxicity demonstrated significant modulation of mitotic cell cycle process, with an up-regulation observed for the majority of the cell cycle-promoting proteins. For years, the precise origins of mitotic dysfunction have not been fully

understood. Cell cycle re-activation association to excitotoxicity has previously been reported on numerous occasions in models of excitotoxicity and stroke, amidst models of other neurodegenerative diseases such as the MPTP model of Parkinson's disease (PD) and superoxide dismutase-1 mouse model of amyotropic lateral sclerosis (ALS) (Hoglinger et al., 2007; Nguyen et al., 2003; Verdaguer et al., 2003,2004a), indicating a similar neuropathological incidence between these two cellular events which may not be a coincidence. Importantly, our study employing a comparative temporal microarray technique demonstrated that iGluR activation plays an important role in the trigger of cell cycle re-activation during Glu-mediated excitotoxicity, and that downstream signaling via iGluRs may be the origin or an important part of the cause of mitotic dysfunction.

Aberrant expression of neuronal cell cycle proteins with resultant neuronal loss has been observed in post-mortem tissue from patients with neurodegenerative diseases such as AD, PD, ALS, DS and progressive supranuclear palsy (Nunomura et al., 2007; Woods et al., 2007) and acute neurological disorder such as stroke and TBI (Byrnes and Faden, 2007; Timsit and Menn, 2007). Accumulating evidence has demonstrated aberrant expression of cell-cycle-related molecules in the neurons of the hippocampus, subiculum, locus coeruleus and dorsal raphe nuclei. Our novel evidence is further substantiated by proof of DNA replication in brains of patients with AD (Busser et al., 1998; McShea et al., 1997; Vincent et al., 1997; Yang et al., 2001), epilepsy (Nagy and Esiri, 1998), PD (Jordan-Sciutto et al., 2003) and ALS (Ranganathan and Bowser, 2003).

Neurons in the adult central nervous system exist in the quiescent state i.e. a non-dividing, silent phase, called G_0. Cells in this state are designated as terminally differentiated as they do not have the ability to re-enter cell cycle (McShea et al., 1999). Increasing evidence from neurodegenerative

diseases studies demonstrates that these mitotically inactive neurons often become the vulnerable targets of aberrant cell cycle re-entry (Lee et al., 2009; McShea et al., 2007; Zhu et al., 1999, 2007). It is likely that under the influence of over-activated iGluRs during excitoxicity, re-entrant neurons that proceed beyond the late G_1, or even enter and complete S-phase, cannot return to G_0. As a result of some undefined cellular constraints of terminally differentiated neurons, the cell cycle re-entrant cells being neither able to return to quiescent state or complete mitosis, induce their own deaths via programmed cell death pathways (Meikrantz and Schlegel, 1995; Wang et al., 2009). Such a fate was evident from the elevated level of pro-apoptotic genes and concomitant down regulation of anti-apoptotic genes as highlighted previously. During cell transitions from S-phase to M-phase in mitosis, cyclins and their associated cyclin-dependent kinases (CDKs), fluctuate in their expression and activity (Grana and Reddy, 1995). In particular, the expression and activation of cyclin D/CDK4,6 complex, triggered by the presence of mitotic growth factors, facilitates the passing from resting (G_0) cells into the G_1 phase of cell cycle (Sherr, 1994, 1995). Similarly, the G_1/S transition is governed by the activation of the cyclin E/CDK2 complex (Sherr, 1994), such that the absence of cyclin E and/or the inhibition of the cyclin E/CDK2 complex by p21, p27 and p53 would impose cell cycle arrest at the G_1 checkpoint.

From profiling the genes involved in mitotic cell division for individual excitotoxicity (Table 2), it is apparent that numerous cell cycle-promoting proteins were transcriptionally up-regulated from 5h and 15h. This finding is in agreement with an increase in gene expression of pro-mitogenic signals from growth factors. Interestingly, transcriptional up-regulation of cyclin D1 and D2 was observed in AMPA and KA models, but not in the NMDA and Glu models. This difference in temporal modulation of cyclin D could be explained by the earlier occurrence of cell cycle re-activation before

the selected 5h time-points in NMDA and Glu profile as a result of the highest physiological abundance and calcium ion permeability of NMDARs out of the three iGluRs subtypes, which leads to the failure to capture the timeframe of cyclin D transcriptional modulation. As such, NMDA profiling demonstrated basal fold-change (~1.0) at 5h, followed by significant pursuing down-regulation at 15h and 24h. On the other hand, L-cyclin D (Ccnd) transcriptional regulation was not present in the Glu profile, indicating an overall close to basal (between -1.50 to 1.50 fold) expression due to a neutralizing effect from the up and down-regulation of Ccnd in AMPA/KA and NMDA profiles respectively upon all iGluRs activation.

While activation of iGluRs during excitotoxicity may be the trigger for the initiation of cell cycle reactivation, oxidative stress may further facilitate and promote its progression (Bonda et al., 2010). Indeed, significant oxidative load, represented by the substantial transcriptional activation of Hsps, molecular chaperones and GSH pathway associated genes, was observed across all four excitotoxicity models. Oxidative stress in particular has been strongly linked to excitotoxic neuronal cell death in both multiple sclerosis and brain ischemia (Gonsette, 2008; Warner et al., 2004). Intriguingly, our study highlights that a "two-hit" hypothesis, originally put forward for neurodegeneration in AD, involves both oxidative stress and aberrant cell cycle activation may apply to neuronal excitotoxicity (Zhu et al., 2001, 2007). In the current study, apart from oxidative stress, the two conditions paramount for aberrant cell cycle re-entry occur in neurons, namely (a) an elevation in cell cycle proteins and (b) an increase in pro-mitogenic signals, have been fulfilled. Even though mature neurons may express some cell cycle proteins, the amount produced is not sufficient to produce a substantial pro-mitogenic signal to drive the mature neuron to re-enter the cell cycle. Furthermore, some cell cycle proteins demonstrate diverse post-mitotic multi-functions that span various developmental stages of a neuron, including neuronal migration, axonal elongation, axonal

pruning, dendrite morphogenesis and synaptic maturation, and plasticity (Frank and Tsai, 2009; Kim et al., 2009). As such, neuronal cell death requires the additional stimulus of pro-mitogenic molecules, such as thrombin, Aβ, ROS, nitric oxide and elevations in the level of such molecules will then trigger the mitogenic signaling cascades in injured neurons. Once mitogenic signaling is stimulated beyond a certain threshold, neurons appear to exit their quiescent state and re-enter the cell cycle and this "vulnerable" state eventually leads to their demise (Bonda et al., 2010).

To date, preclinical experiments employing inhibitors (flavopiridol, olomoucine or roscovitine) of cell cycle protein kinase family, CDKs, demonstrate improved behavioral outcomes and increased neuronal survival in a series of CNS disease models such as AD (Copani et al., 2001; Jorda et al., 2003; Verdaguer et al., 2004b), PD (Kruman and Schwartz, 2006), stroke (Osuga et al., 2000; Wang et al., 2002) and TBI (Hilton et al., 2008). All of these neuropathologies are believed to involve iGluR-mediated excitotoxicity and there is a literature suggesting inhibitors of CDKs are neuroprotective against excitotoxicity (Giardinia and Beart, 2002). Overall, our gene profiling indicate that oxidative stress and cell cycle re-entry are primary events taking place during iGluR overactivation in neurons and further support the "two-hit" hypothesis for excitotoxic neuronal cell death. More importantly, our study suggests that a combined therapeutic approach using drugs that salvage oxidative stress and prevent the onset of cell cycle may potentially delay death and provide neurons with "bonus" time for recovery during excitotoxicity associated with multiple neurodegenerative diseases.

5. Acknowledgement

This work is supported by: NSC and PMB, project grant funding from the National Health and Medical Research Council of Australia. PMB is a Research Fellow of the NHMRC (Australia).

6. References

Arundine, M., Tymianski, M., 2003. Molecular mechanisms of calcium-dependent neurodegeneration in excitotoxicity. Cell Calcium 34, 325-337.

Arundine, M., Tymianski, M., 2004. Molecular mechanisms of glutamate-dependent neurodegeneration in ischemia and traumatic brain injury. Cell Mol Life Sci 61, 657-668.

Bassani, S., Valnegri, P., Beretta, F., Passafaro, M., 2009. The GLUR2 subunit of AMPA receptors: synaptic role. Neuroscience 158, 55-61.

Beart, P.M., O'Shea, R.D., 2007. Transporters for L-glutamate: an update on their molecular pharmacology and pathological involvement. Br J Pharmacol 150, 5-17.

Bonda, D.J., Bajic, V.P., Spremo-Potparevic, B., Casadesus, G., Zhu, X., Smith, M.A., Lee, H.G., 2010. Review: cell cycle aberrations and neurodegeneration. Neuropathol Appl Neurobiol 36, 157-163.

Busser, J., Geldmacher, D.S., Herrup, K., 1998. Ectopic cell cycle proteins predict the sites of neuronal cell death in Alzheimer's disease brain. J Neurosci 18, 2801-2807.

Byrnes, K.R., Faden, A.I., 2007. Role of cell cycle proteins in CNS injury. Neurochem Res 32, 1799-1807.

Camins, A., Pallas, M., Silvestre, J.S., 2008. Apoptotic mechanisms involved in neurodegenerative diseases: experimental and therapeutic approaches. Methods Find Exp Clin Pharmacol 30, 43-65.

Cheung, N.S., Carroll, F.Y., Larm, J.A., Beart, P.M., Giardina, S.F., 1998. Kainate-induced apoptosis correlates with c-Jun activation in cultured cerebellar granule cells. J Neurosci Res 52, 69-82.

Cheung, N.S., Beart, P.M., Pascoe, C.J., John, C.A., Bernard, O., 2000. Human Bcl-2 protects against AMPA receptor-mediated apoptosis. J Neurochem 74, 1613-1620.

Cheung, N.S., Peng, Z.F., Chen, M.J., Moore, P.K., Whiteman, M., 2007. Hydrogen sulfide induced neuronal cell death occurs via glutamate receptor and is associated with calpain activation and lysosomal rupture in mouse primary cortical neurons. Neuropharmacology, 53, 505-514.

Copani, A., Uberti, D., Sortino, M.A., Bruno, V., Nicoletti, F., Memo, M., 2001. Activation of cell-cycle-associated proteins in neuronal death: a mandatory or dispensable path? Trends Neurosci 24, 25-31.

Costa, M.S., Rocha, J.B., Perosa, S.R., Cavalheiro, E.A., Naffah-Mazzacoratti Mda, G., 2004. Pilocarpine-induced status epilepticus increases glutamate release in rat hippocampal synaptosomes. Neurosci Lett 356, 41-44.

Dennis, G., Jr., Sherman, B.T., Hosack, D.A., Yang, J., Gao, W., Lane, H.C. Lempicki, R.A., 2003. DAVID: Database for annotation, visualization, and integrated discovery. Genome Biol 4, P3.

Ding, S., Fellin, T., Zhu, Y., Lee, S.Y., Auberson, Y.P., Meaney, D.F., Coulter, D.A., Carmignoto, G., Haydon, P.G., 2007. Enhanced astrocytic Ca2+ signals contribute to neuronal excitotoxicity after status epilepticus. J Neurosci 27, 10674-10684.

Doble, A., 1999. The role of excitotoxicity in neurodegenerative disease: implications for therapy. Pharmacol Ther 81, 163-221.

Frank, C.L., Tsai, L.H., 2009. Alternative functions of core cell cycle regulators in neuronal migration, neuronal maturation, and synaptic plasticity. Neuron 62, 312-326.

Giardina, S.F., Beart, P.M., 2002. Kainate receptor-mediated apoptosis in primary cultures of cerebellar granule cells is attenuated by mitogen-activated protein and cyclin-dependent kinase inhibitors. Br J Pharmacol 135, 1733-1742.

Gonsette, R.E., 2008. Oxidative stress and excitotoxicity: a therapeutic issue in multiple sclerosis? Mult Scler 14, 22-34.

Graber, S., Maiti, S., Halpain, S., 2004. Cathepsin B-like proteolysis and MARCKS degradation in sublethal NMDA-induced collapse of dendritic spines. Neuropharmacol 47, 706-713.

Grana, X., Reddy, E.P., 1995. Cell cycle control in mammalian cells: role of cyclins, cyclin dependent kinases (CDKs), growth suppressor genes and cyclin-dependent kinase inhibitors (CKIs). Oncogene 11, 211-219.

Hara, M.R., Snyder, S.H., 2007. Cell signaling and neuronal death. Annu Rev Pharmacol Toxicol 47, 117-141.

Hilton, G.D., Stoica, B.A., Byrnes, K.R., Faden, A.I., 2008. Roscovitine reduces neuronal loss, glial activation, and neurologic deficits after brain trauma. J Cereb Blood Flow Metab 28, 1845-1859.

Hoglinger, G.U., Breunig, J.J., Depboylu, C., Rouaux, C., Michel, P.P., Alvarez-Fischer, D., Boutillier, A.L., Degregori, J., Oertel, W.H., Rakic, P., Hirsch, E.C., Hunot, S., 2007. The pRb/E2F cell-cycle pathway mediates cell death in Parkinson's disease. Proc Natl Acad Sci U S A 104, 3585-3590.

Huang, D.W., Sherman, B.T., Lempicki, R.A., 2009. Systematic and integrative analysis of large gene lists using DAVID Bioinformatics Resources. Nature Protoc 4, 44-57.

Hynd, M.R., Scott, H.L., Dodd, P.R., 2004. Differential expression of N-methyl-D-aspartate receptor NR2 isoforms in Alzheimer's disease. J Neurochem 90, 913-919.

Jayakar, S.S., Dikshit, M., 2004. AMPA receptor regulation mechanisms: future target for safer neuroprotective drugs. Int J Neurosci 114, 695-734.

Jorda, E.G., Verdaguer, E., Canudas, A.M., Jimenez, A., Bruna, A., Caelles, C., Bravo, R., Escubedo, E., Pubill, D., Camarasa, J., Pallas, M., Camins, A., 2003. Neuroprotective action of flavopiridol, a cyclin-dependent kinase inhibitor, in colchicine-induced apoptosis. Neuropharmacology 45, 672-683.

Jordan-Sciutto, K.L., Dorsey, R., Chalovich, E.M., Hammond, R.R., Achim, C.L., 2003. Expression patterns of retinoblastoma protein in Parkinson disease. J Neuropathol Exp Neurol 62, 68-74.

Kim, A.H., Puram, S.V., Bilimoria, P.M., Ikeuchi, Y., Keough, S., Wong, M., Rowitch, D., Bonni, A., 2009. A centrosomal Cdc20-APC pathway controls dendrite morphogenesis in postmitotic neurons. Cell 136, 322-336.

Kruman, I., Schwartz, E., 2006. Methods of neuroprotection by cyclin-dependent kinase inhibition. US 20080182853.

Larm, J.A., Cheung, N.S., Beart, P.M., 1997. Apoptosis induced via AMPA-selective glutamate receptors in cultured murine cortical neurons. J Neurochem 69, 617-622.

Lea, P.M. 4th, Faden, A.I., 2003. Modulation of metabotropic glutamate receptors as potential treatment for acute and chronic neurodegenerative disorders. Drug News Perspect 16, 513-522.

Lee, H.G., Casadesus, G., Zhu, X., Castellani, R.J., McShea, A., Perry, G., Petersen, R.B., Bajic, V., Smith, M.A., 2009. Cell cycle re-entry mediated neurodegeneration and its treatment role in the pathogenesis of Alzheimer's disease. Neurochem Int 54, 84-88.

Lopes, J.P., Blurton-Jones, M., Yamasaki, T.R., Agostinho, P., LaFerla, F.M., 2009a. Activation of cell cycle proteins in transgenic mice in response to neuronal loss but not amyloid-beta and tau pathology. J Alzheimers Dis 16, 541-549.

Lopes, J.P., Oliveira, C.R., Agostinho, P., 2009b. Cell cycle re-entry in Alzheimer's disease: a major neuropathological characteristic? Curr Alzheimer Res 6, 205-212.

McShea, A., Harris, P.L., Webster, K.R., Wahl, A.F., Smith, M.A., 1997. Abnormal expression of the cell cycle regulators P16 and CDK4 in Alzheimer's disease. Am J Pathol 150, 1933-1939.

McShea, A., Lee, H.G., Petersen, R.B., Casadesus, G., Vincent, I., Linford, N.J., Funk, J.O., Shapiro, R.A., Smith, M.A., 2007. Neuronal cell cycle re-entry mediates Alzheimer disease-type changes. Biochim Biophys Acta 1772, 467-472.

McShea, A., Wahl, A.F., Smith, M.A., 1999. Re-entry into the cell cycle: a mechanism for neurodegeneration in Alzheimer disease. Med Hypotheses 52, 525-527.

Meikrantz, W., Schlegel, R., 1995. Apoptosis and the cell cycle. J Cell Biochem 58, 160-174.

Mukherjee, S., Manahan-Vaughan, D., 2012. Role of metabotropic glutamate receptors in persistent forms of hippocampal plasticity and learning. Neuropharmacology. [Epub ahead of print]

Nagy, Z., Esiri, M.M., 1998. Neuronal cyclin expression in the hippocampus in temporal lobe epilepsy. Exp Neurol 150, 240-247.

Nguyen, M.D., Boudreau, M., Kriz, J., Couillard-Despres, S., Kaplan, D.R., Julien, J.P., 2003. Cell cycle regulators in the neuronal death pathway of amyotrophic lateral sclerosis caused by mutant superoxide dismutase 1. J Neurosci 23, 2131-2140.

Niciu, M.J., Kelmendi, B., Sanacora, G., 2012. Overview of glutamatergic neurotransmission in the nervous system. Pharmacol Biochem Behav 100, 656-664.

Nunomura, A., Moreira, P.I., Lee, H.G., Zhu, X., Castellani, R.J., Smith, M.A., Perry, G., 2007. Neuronal death and survival under oxidative stress in Alzheimer and Parkinson diseases. CNS Neurol Disord Drug Targets 6, 411-423.

Osuga, H., Osuga, S., Wang, F., Fetni, R., Hogan, M.J., Slack, R.S., Hakim, A.M., Ikeda, J.E., Park, D.S., 2000. Cyclin-dependent kinases as a therapeutic target for stroke. Proc Natl Acad Sci USA 97, 10254-10259.

Pelegri, C., Duran-Vilaregut, J., del Valle, J., Crespo-Biel, N., Ferrer, I., Pallas, M., Camins, A., Vilaplana, J., 2008. Cell cycle activation in striatal neurons from Huntington's disease patients and rats treated with 3-nitropropionic acid. Int J Dev Neurosci 26, 665-671.

Posner, A., Raser, K.J., Hajimohammadreza, I., Yuen, P.W., Wang, K.K., 1995. Aurintricarboxylic acid is an inhibitor of mu- and m-calpain. Biochem Mol Biol Int 36, 291-299.

Ranganathan, S., Bowser, R., 2003. Alterations in G(1) to S phase cell-cycle regulators during amyotrophic lateral sclerosis. Am J Pathol 162, 823-835.

Sattler, R., Tymianski, M., 2001. Molecular mechanisms of glutamate receptor-mediated excitotoxic neuronal cell death. Mol Neurobiol 24, 107-129.

Scheuer, K., Maras, A., Gattaz, W.F., Cairns, N., Forstl, H., Muller, W.E., 1996. Cortical NMDA receptor properties and membrane fluidity are altered in Alzheimer's disease. Dementia 7, 210-214.

Sherr, C.J., 1994. G1 phase progression: cycling on cue. Cell 79, 551-555.

Sherr, C.J., 1995. D-type cyclins. Trends Biochem Sci 20, 187-190.

Siman, R., Noszek, J.C., Kegerise, C., 1989. Calpain I activation is specifically related to excitatory amino acid induction of hippocampal damage. J Neurosci 9, 1579-1590.

Simpkins, K.L., Guttmann, R.P., Dong, Y., Chen, Z., Sokol, S., Neumar, R.W., Lynch, D.R., 2003. Selective activation induced cleavage of the NR2B subunit by calpain. J Neurosci 23, 11322-11331.

Tenneti, L., D'Emilia, D.M., Troy, C.M., Lipton, S.A., 1998. Role of caspases in N-methyl-D-aspartate-induced apoptosis in cerebrocortical neurons. J Neurochem 71, 946-959.

Timsit, S., Menn, B., 2007. Cerebral ischemia, cell cycle elements and Cdk5. Biotechnol J 2, 958-966.

Verdaguer, E., Jimenez, A., Canudas, A.M., Jorda, E.G., Sureda, F.X., Pallas, M., Camins, A., 2004a. Inhibition of cell cycle pathway by flavopiridol promotes survival of cerebellar granule cells after an excitotoxic treatment. J Pharmacol Exp Ther 308, 609-616.

Verdaguer, E., Jorda, E.G., Canudas, A.M., Jimenez, A., Pubill, D., Escubedo, E., Camarasa, J., Pallas, M., Camins, A., 2004b. Antiapoptotic effects of roscovitine in cerebellar granule cells deprived of serum and potassium: a cell cycle-related mechanism. Neurochem Int 44, 251-261.

Verdaguer, E., Jorda, E.G., Canudas, A.M., Jimenez, A., Sureda, F.X., Rimbau, V., Pubill, D., Escubedo, E., Camarasa, J., Pallas, M., Camins, A., 2003. 3-Amino thioacridone, a selective cyclin-dependent kinase 4 inhibitor, attenuates kainic acid-induced apoptosis in neurons. Neuroscience 120, 599-603.

Vincent, I., Jicha, G., Rosado, M., Dickson, D.W., 1997. Aberrant expression of mitotic cdc2/cyclin B1 kinase in degenerating neurons of Alzheimer's disease brain. J Neurosci 17, 3588-3598.

Vincent, P., Mulle, C., 2009. Kainate receptors in epilepsy and excitotoxicity. Neuroscience 158, 309-323.

Wang, F., Corbett, D., Osuga, H., Osuga, S., Ikeda, J.E., Slack, R.S., Hogan, M.J., Hakim, A.M., Park, D.S., 2002. Inhibition of cyclin-dependent kinases improves CA1 neuronal survival and behavioral performance after global ischemia in the rat. J Cereb Blood Flow Metab 22, 171-182.

Wang, W., Bu, B., Xie, M., Zhang, M., Yu, Z., Tao, D., 2009. Neural cell cycle dysregulation and central nervous system diseases. Prog Neurobiol 89, 1-17.

Warner, D.S., Sheng, H., Batinic-Haberle, I., 2004. Oxidants, antioxidants and the ischemic brain. J Exp Biol 207, 3221-3231.

Wieloch, T., Engelsen, B., Westerberg, E., Auer, R., 1985. Lesions of the glutamatergic cortico-striatal projections in the rat ameliorate hypoglycemic brain damage in the striatum. Neurosci Lett 58, 25-30.

Woods, J., Snape, M., Smith, M.A., 2007. The cell cycle hypothesis of Alzheimer's disease: suggestions for drug development. Biochim Biophys Acta 1772, 503-508.

Wright, A., Vissel, B., 2012. The essential role of AMPA receptor GluR2 subunit RNA editing in the normal and diseased brain. Front Mol Neurosci 5, 34.

Yang, Y., Geldmacher, D.S., Herrup, K., 2001. DNA replication precedes neuronal cell death in Alzheimer's disease. J Neurosci 21, 2661-2668.

Zhu, X., Castellani, R.J., Takeda, A., Nunomura, A., Atwood, C.S., Perry, G., Smith, M.A., 2001. Differential activation of neuronal ERK, JNK/SAPK and p38 in Alzheimer disease: the 'two hit' hypothesis. Mech Ageing Dev 123, 39-46.

Zhu, X., Lee, H.G., Perry, G., Smith, M.A., 2007. Alzheimer disease, the two-hit hypothesis: an update. Biochim Biophys Acta 1772, 494-502.

Zhu, X., Raina, A.K., Perry, G., Smith, M.A., 2004. Alzheimer's disease: the two-hit hypothesis. Lancet Neurol 3, 219-226.

Zhu, X., Raina, A.K., Smith, M.A., 1999. Cell cycle events in neurons. Proliferation or death? Am J Pathol 155, 327-329.

7. Conflict of interest

The authors declare that they have no conflict of interest.

8. Figure Legends

Figure 1. Classification of individual iGluRs global transcriptomic profiles (passed microarray selection criteria: total numbers of genes showing expression at least ±1.5 fold change in a minimum of one out of the three time-points (5h, 15h and 24h) and statistical examination using one-way ANOVA, $p < 0.05$ and Benjamini-Hochberg FDR) according to specific time-points and fold-change expression up/down-regulated.

Figure 2. Bi-model global transcriptomic profile analysis of individual iGluRs agonists against Glu excitotoxic model. Venn diagrams demonstrating the number of gene probes common and mutually exclusive to both models [A] Glu against NMDA [B] Glu against AMPA and [C] Glu against KA.

Figure 3. Consistency in the transcriptional regulatory trend of the commonly occurring and significantly modulated gene probes in individual iGluRs against Glu excitotoxic models.

Figure 4. Overall consistency in the transcriptional regulatory trend of the commonly occurring and significantly modulated gene probes [A] at respective time-points (5h, 15h and 24h) and [B] across all three time points in all four excitotoxic models.

9. Tables

Table 1. Gene expression profiles of neuronal death-related families in cultured mouse primary cortical neurons treated with EC_{50} concentrations of AMPA, KA, NMDA and Glu over a 24-hour period respectively. All expression values (given as fold-changes) were selected based on having at least minimum of ±1.5 fold change in at least one out of three time-points, subjected to one-way ANOVA analysis and were significant at $p < 0.05$. Values are given as mean ± sem.

			Time-points											
			300 µM AMPA			100 µM KA			200 µM NMDA			250 µM Glu		
Genbank	**Gene Title**	**Symbol**	**5h**	**15h**	**24h**	**5h**	**15h**	**24h**	**5h**	**15h**	**24h**	**5h**	**15h**	**24h**
Calcium ion homeostasis and binding														
NM_008151	G-protein coupled receptor 12	Gpr12	-2.40 ± 0.09	-1.70 ± 0.15	-1.80 ± 0.14	-2.18 ± 0.13	-2.66 ± 0.12	-2.89 ± 0.11	-1.50 ± 0.19	-2.20 ± 0.11	-2.00 ± 0.13	-1.43 ± 0.19	-1.80 ± 0.17	-1.40 ± 0.18
NM_007587	Calcitonin/calcitonin-related polypeptide, alpha	Calca	1.10 ± 0.36	1.50 ± 0.47	1.20 ± 0.34	1.11 ± 0.40	2.17 ± 0.47	2.15 ± 0.67	1.10 ± 0.35	1.90 ± 0.54	1.64 ± 0.43	-1.10 ± 0.31	2.30 ± 0.66	2.80 ± 0.71
NM_008855	Protein kinase C, beta 1	Prkcb	-1.10 ± 0.21	-1.72 ± 0.16	-1.94 ± 0.12	-1.04 ± 0.27	-1.82 ± 0.12	-2.40 ± 0.12	-1.20 ± 0.26	-2.80 ± 0.09	-2.50 ± 0.09	-1.10 ± 0.23	-1.60 ± 0.12	-1.38 ± 0.18
NM_011313	S100 calcium binding protein A6 (calcyclin)	S100a6	1.17 ± 0.23	1.65 ± 0.36	1.10 ± 0.19	1.35 ± 0.24	2.12 ± 0.39	1.66 ± 0.30	1.50 ± 0.29	2.80 ± 0.51	2.22 ± 0.35	1.00 ± 0.18	1.93 ± 0.38	1.90 ± 0.37
NM_007585	Annexin A2	Anxa2	1.99 ± 0.38	1.80 ± 0.42	1.38 ± 0.31	2.30 ± 0.45	1.98 ± 0.34	1.48 ± 0.35	1.90 ± 0.38	2.24 ± 0.43	1.60 ± 0.31	1.52 ± 0.25	1.93 ± 0.31	2.05 ± 0.43
NM_013470	Annexin A3	Anxa3	1.30 ± 0.30	1.89 ± 0.48	1.66 ± 0.58	1.00 ± 0.23	1.95 ± 0.43	1.61 ± 0.42	1.50 ± 0.45	3.14 ± 0.77	2.60 ± 0.58	1.20 ± 0.31	3.60 ± 0.81	3.20 ± 0.63
NM_009673	Annexin A5	Anxa5	-1.00 ± 0.23	1.50 ± 0.31	1.10 ± 0.24	-1.00 ± 0.19	1.50 ± 0.33	1.10 ± 0.21	1.40 ± 0.27	2.00 ± 0.40	1.80 ± 0.35	1.20 ± 0.20	1.70 ± 0.29	1.60 ± 0.38

			Time-points											
			300µM AMPA			100µM KA			200µM NMDA			250µM Glu		
Genbank	**Gene Title**	**Symbol**	**5h**	**15h**	**24h**	**5h**	**15h**	**24h**	**5h**	**15h**	**24h**	**5h**	**15h**	**24h**
Lysosomal stress														
NM_017372	Lysozyme 2	Lyz2	1.63 ± 0.40	1.42 ± 0.36	-1.13 ± 0.24	-1.10 ± 0.29	1.50 ± 0.36	1.40 ± 0.43	1.60 ± 0.61	2.10 ± 0.69	2.10 ± 0.48	1.20 ± 0.30	1.65 ± 0.40	1.50 ± 0.44
NM_010686	Lysosomal-associated protein transmembrane 5	Laptm5	1.70 ± 0.31	1.40 ± 0.34	-1.10 ± 0.19	-1.50 ± 0.18	1.80 ± 0.34	1.40 ± 0.50	1.71 ± 0.46	2.31 ± 0.98	2.13 ± 0.34	1.34 ± 0.25	1.98 ± 0.37	1.95 ± 0.40
NM_010685	Lysosomal-associated membrane protein 2	Lamp2	1.38 ± 0.39	1.60 ± 0.41	1.30 ± 0.32	1.63 ± 0.39	2.23 ± 0.50	1.54 ± 0.37	1.44 ± 0.36	2.31 ± 0.41	1.77 ± 0.30	-1.10 ± 0.30	1.75 ± 0.51	1.70 ± 0.38
NM_019972	Sortilin 1	Sort1	1.10 ± 0.35	1.28 ± 0.50	1.22 ± 0.54	1.50 ± 0.51	2.31 ± 0.56	1.80 ± 0.46	1.50 ± 0.45	3.70 ± 0.81	2.50 ± 0.64	1.50 ± 0.45	2..00 ± 0.63	1.40 ± 0.44
NM_009906	Tripeptidyl peptidase I	Tpp1	1.20 ± 0.29	1.70 ± 0.53	1.10 ± 0.30	1.50 ± 0.40	1.95 ± 0.53	1.70 ± 0.54	1.20 ± 0.36	1.70 ± 0.40	1.30 ± 0.31	-1.10 ± 0.32	1.60 ± 0.41	1.60 ± 0.40
Anti-oxidant response - Heat shock proteins and molecular chaperones														
NM_010442	Heme oxygenase (decycling) 1	Hmox1	2.32 ± 0.45	1.68 ± 0.29	1.38 ± 0.51	2.34 ± 0.39	2.17 ± 0.39	2.04 ± 0.37	2.70 ± 0.58	3.11 ± 0.48	1.60 ± 0.29	1.60 ± 0.34	2.37 ± 0.41	1.51 ± 0.38
NM_029688	Sulfiredoxin 1 homolog (S. cerevisiae)	Srxn1	2.60 ± 0.56	1.70 ± 0.34	1.30 ± 0.41	3.10 ± 0.54	1.93 ± 0.36	1.38 ± 0.30	2.00 ± 0.39	1.95 ± 0.28	1.10 ± 0.19	-1.20 ± 0.29	2.16 ± 0.73	1.17 ± 0.43
NM_007453	Peroxiredoxin 6	Prdx6	1.32 ± 0.41	1.72 ± 0.55	1.16 ± 0.37	1.10 ± 0.30	1.30 ± 0.30	1.25 ± 0.40	1.14 ± 0.36	1.62 ± 0.47	1.20 ± 0.28	-1.10 ± 0.27	2.02 ± 0.60	1.80 ± 0.56
NM_008301	Heat shock protein 2	Hspa2	1.50 ± 0.44	3.00 ± 0.76	2.30 ± 0.64	1.64 ± 0.44	2.77 ± 0.65	2.26 ± 0.64	1.00 ± 0.26	2.00 ± 0.52	2.00 ± 0.47	-1.30 ± 0.19	1.64 ± 0.36	1.60 ± 0.39
NM_030704	Heat shock protein 8	Hspb8	1.80 ± 0.45	2.20 ± 0.63	1.40 ± 0.59	1.42 ± 0.37	2.61 ± 0.59	1.60 ± 0.38	2.00 ± 0.46	3.90 ± 0.80	1.83 ± 0.46	1.29 ± 0.31	4.40 ± 1.06	2.63 ± 0.70
NM_013602	Metallothionein 1	Mt1	1.56 ± 0.28	1.74 ± 0.28	1.21 ± 0.17	2.00 ± 0.40	2.29 ± 0.38	1.92 ± 0.38	1.60 ± 0.25	2.00 ± 0.34	1.50 ± 0.24	1.10 ± 0.16	1.80 ± 0.26	1.80 ± 0.39
NM_013603	Metallothionein 3	Mt3	1.49 ± 0.26	1.80 ± 0.69	1.10 ± 0.20	2.34 ± 0.48	1.90 ± 0.34	2.00 ± 0.49	1.35 ± 0.27	1.90 ± 0.27	1.80 ± 0.55	-1.10 ± 0.17	1.60 ± 0.28	1.60 ± 0.30

			Time-points											
			300µM AMPA			100µM KA			200µM NMDA			250µM Glu		
Genbank	**Gene Title**	**Symbol**	**5h**	**15h**	**24h**	**5h**	**15h**	**24h**	**5h**	**15h**	**24h**	**5h**	**15h**	**24h**
Anti-oxidant response - Glutathione metabolism														
NM_010357	Glutathione S-transferase, alpha 4	Gsta4	1.10 ± 0.29	1.82 ± 0.44	1.40 ± 0.33	1.14 ± 0.31	2.30 ± 0.60	2.03 ± 0.48	1.30 ± 0.39	3.05 ± 0.70	2.14 ± 0.52	-1.20 ± 0.18	2.60 ± 0.63	2.10 ± 0.59
NM_008184	Glutathione S-transferase, mu 6	Gstm6	1.20 ± 0.40	1.50 ± 0.53	-1.00 ± 0.35	1.50 ± 0.50	1.90 ± 0.52	1.20 ± 0.36	1.45 ± 0.45	2.10 ± 0.63	1.34 ± 0.35	-1.20 ± 0.22	2.10 ± 0.58	1.70 ± 0.52
NM_019946	Microsomal glutathione S-transferase 1	Mgst1	1.10 ± 0.30	1.80 ± 0.46	1.30 ± 0.42	1.40 ± 0.44	2.55 ± 0.53	1.91 ± 0.51	1.71 ± 0.42	2.96 ± 0.60	1.67 ± 0.37	-1.00 ± 0.27	3.20 ± 0.87	2.90 ± 0.90
NM_025569	Microsomal glutathione S-transferase 3	Mgst3	-1.25 ± 0.19	-1.56 ± 0.15	-1.40 ± 0.16	-1.20 ± 0.20	-2.26 ± 0.09	-2.14 ± 0.12	-1.25 ± 0.18	-2.00 ± 0.10	-1.63 ± 0.12	-1.30 ± 0.14	-1.70 ± 0.11	-1.60 ± 0.12
NM_010358	Glutathione S-transferase, mu 1	Gstm1	1.30 ± 0.26	1.68 ± 0.27	1.10 ± 0.18	1.57 ± 0.33	2.12 ± 0.40	1.42 ± 0.40	1.45 ± 0.32	2.23 ± 0.46	1.43 ± 0.30	-1.10 ± 0.14	1.90 ± 0.37	1.64 ± 0.35
Cell death														
NM_020581	Angiopoietin-like 4	Angptl4	2.70 ± 0.59	5.32 ± 1.14	2.36 ± 0.63	4.74 ± 0.84	11.98 ± 2.14	10.21 ± 2.28	3.42 ± 0.65	7.93 ± 1.61	5.32 ± 1.00	2.00 ± 0.46	8.27 ± 1.62	8.24 ± 1.58
NM_009811	Caspase 6	Casp6	1.10 ± 0.28	1.60 ± 0.33	1.20 ± 0.32	1.30 ± 0.30	2.10 ± 0.35	1.60 ± 0.36	1.50 ± 0.39	2.42 ± 0.48	1.74 ± 0.27	1.20 ± 0.31	2.00 ± 0.37	1.70 ± 0.46
NM_009818	Catenin (cadherin associated protein), alpha 1	Ctnna1	1.30 ± 0.21	1.55 ± 0.24	1.20 ± 0.18	1.30 ± 0.23	2.10 ± 0.29	1.43 ± 0.27	1.55 ± 0.28	2.40 ± 0.33	1.80 ± 0.32	1.20 ± 0.20	1.90 ± 0.34	1.80 ± 0.36
NM_021399	B-cell leukemia/lymphoma 11B	Bcl11b	-1.07 ± 0.17	-1.80 ± 0.11	-1.60 ± 0.12	-1.37 ± 0.16	-1.53 ± 0.12	-1.82 ± 0.11	-1.00 ± 0.21	-2.20 ± 0.09	-1.80 ± 0.11	1.00 ± 0.17	-1.70 ± 0.10	-1.50 ± 0.12

			Time-points											
			300µM AMPA			100µM KA			200µM NMDA			250µM Glu		
Genbank	**Gene Title**	**Symbol**	**5h**	**15h**	**24h**	**5h**	**15h**	**24h**	**5h**	**15h**	**24h**	**5h**	**15h**	**24h**
Cell homeostasis, survival and proliferation														
NM_010835	Homeobox, msh-like 1	Msx1	1.17 ± 0.35	1.65 ± 0.48	1.00 ± 0.29	1.90 ± 0.63	2.02 ± 0.54	1.82 ± 0.46	1.25 ± 0.33	1.60 ± 0.34	1.45 ± 0.36	-1.30 ± 0.25	1.90 ± 0.57	1.80 ± 0.47
NM_152229	Nuclear receptor subfamily 2, group E, member 1	Nr2e1	1.40 ± 0.28	1.80 ± 0.38	1.30 ± 0.29	1.90 ± 0.40	2.30 ± 0.42	1.70 ± 0.35	1.40 ± 0.35	2.00 ± 0.32	1.60 ± 0.50	1.00 ± 0.21	2.00 ± 0.48	2.10 ± 0.47
NM_009263	Secreted phosphoprotein 1	Spp1	1.77 ± 0.40	1.55 ± 0.38	1.03 ± 0.28	-1.00 ± 0.32	2.43 ± 0.68	2.23 ± 0.67	1.90 ± 0.83	3.50 ± 3.20	4.30 ± 1.17	1.20 ± 0.30	2.00 ± 0.44	2.00 ± 0.45
NM_009129	Secretogranin II	Scg2	10.12 ± 2.32	11.74 ± 2.39	9.17 ± 1.77	11.00 ± 2.47	14.06 ± 2.73	12.03 ± 1.93	1.94 ± 0.44	2.44 ± 0.82	4.03 ± 0.85	1.00 ± 0.22	-4.09 ± 0.07	-3.79 ± 0.08
NM_009696	Apolipoprotein E	Apoe	1.09 ± 0.23	1.70 ± 0.29	1.30 ± 0.24	1.30 ± 0.28	2.36 ± 0.43	1.98 ± 0.36	1.15 ± 0.27	2.40 ± 0.52	1.80 ± 0.27	-1.20 ± 0.14	1.70 ± 0.32	1.70 ± 0.37
NM_009689	Baculoviral IAP repeat-containing 5	Birc5	1.94 ± 0.50	1.25 ± 0.37	-1.00 ± 0.26	2.09 ± 0.59	1.39 ± 0.35	1.21 ± 0.31	2.00 ± 0.56	1.40 ± 0.33	-1.00 ± 0.22	1.54 ± 0.36	1.88 ± 0.50	1.34 ± 0.30
NM_013863	Bcl2-associated athanogene 3	Bag3	1.80 ± 0.24	2.40 ± 0.39	2.40 ± 0.48	2.50 ± 0.37	2.49 ± 0.37	2.09 ± 0.31	2.30 ± 0.47	2.70 ± 0.36	2.50 ± 0.48	1.60 ± 0.34	2.00 ± 0.38	1.80 ± 0.45
NM_010514	Insulin-like growth factor 2	Igf2	1.40 ± 0.28	1.50 ± 0.30	1.00 ± 0.21	1.80 ± 0.35	2.10 ± 0.43	1.60 ± 0.39	1.60 ± 0.36	1.70 ± 0.41	1.30 ± 0.28	1.60 ± 0.32	2.40 ± 0.52	2.10 ± 0.52
NM_133662	Immediate early response 3	Ier3	1.40 ± 0.32	1.40 ± 0.37	1.80 ± 0.45	-1.00 ± 0.26	1.60 ± 0.31	1.60 ± 0.35	1.20 ± 0.32	1.70 ± 0.31	1.60 ± 0.27	1.90 ± 0.48	1.10 ± 0.34	1.00 ± 0.21
NM_008520	Latent transforming growth factor beta binding protein 3	Ltbp3	1.10 ± 0.25	1.80 ± 0.43	1.60 ± 0.32	1.05 ± 0.33	1.23 ± 0.41	1.38 ± 0.41	1.20 ± 0.26	1.60 ± 0.34	1.80 ± 0.35	-1.00 ± 0.22	1.50 ± 0.25	1.90 ± 0.41
NM_010518	Insulin-like growth factor binding protein 5	Igfbp5	-1.10 ± 0.25	1.60 ± 0.32	1.10 ± 0.26	1.30 ± 0.26	2.14 ± 0.38	1.61 ± 0.40	1.10 ± 0.25	2.00 ± 0.40	1.80 ± 0.39	-1.20 ± 0.12	1.70 ± 0.28	1.90 ± 0.40

			Time-points											
			300μM AMPA			100μM KA			200μM NMDA			250μM Glu		
Genbank	**Gene Title**	**Symbol**	**5h**	**15h**	**24h**	**5h**	**15h**	**24h**	**5h**	**15h**	**24h**	**5h**	**15h**	**24h**
NM_021099	Kit oncogene	Kit	-2.12 ± 0.10	-1.19 ± 0.20	-1.15 ± 0.18	-1.84 ± 0.11	-2.90 ± 0.07	-2.40 ± 0.10	-1.50 ± 0.13	-2.10 ± 0.10	-1.20 ± 0.18	-1.50 ± 0.12	-1.70 ± 0.12	-1.50 ± 0.17
Mitotic cell cycle														
NM_025565	SPC25, NDC80 kinetochore complex component, homolog (S. cerevisiae)	Spc25	1.79 ± 0.52	1.50 ± 0.52	-1.08 ± 0.32	2.40 ± 0.81	1.83 ± 0.57	1.34 ± 0.45	2.11 ± 0.48	1.82 ± 0.49	1.21 ± 0.32	1.66 ± 0.41	1.85 ± 0.65	1.47 ± 0.63
NM_028390	Anillin, actin binding protein	Anln	1.97 ± 0.51	1.28 ± 0.28	-1.10 ± 0.19	1.96 ± 0.48	1.60 ± 0.35	1.19 ± 0.32	1.84 ± 0.41	1.50 ± 0.33	1.18 ± 0.26	1.80 ± 0.40	1.86 ± 0.51	1.67 ± 0.41
NM_011497	Aurora kinase A	Aurka	2.31 ± 0.56	1.48 ± 0.36	1.04 ± 0.25	2.30 ± 0.55	1.46 ± 0.37	1.07 ± 0.29	1.65 ± 0.40	1.31 ± 0.32	1.11 ± 0.26	1.91 ± 0.42	1.98 ± 0.50	1.59 ± 0.44
NM_028109	TPX2, microtubule-associated protein homolog (Xenopus laevis)	Tpx2	1.80 ± 0.46	1.27 ± 0.41	-1.08 ± 0.26	1.90 ± 0.49	1.49 ± 0.45	1.06 ± 0.35	1.80 ± 0.49	1.50 ± 0.33	1.10 ± 0.25	1.70 ± 0.42	2.09 ± 0.55	1.57 ± 0.46
NM_007659	Cyclin-dependent kinase 1	Cdk1	2.58 ± 0.62	1.54 ± 0.45	-1.10 ± 0.26	3.02 ± 0.71	1.74 ± 0.38	1.18 ± 0.32	2.10 ± 0.51	1.66 ± 0.39	1.19 ± 0.26	2.06 ± 0.42	1.91 ± 0.47	1.50 ± 0.39
NM_023223	Cell division cycle 20 homolog (S. cerevisiae)	Cdc20	1.53 ± 0.50	1.06 ± 0.38	-1.15 ± 0.24	1.51 ± 0.55	1.35 ± 0.50	1.04 ± 0.46	1.87 ± 0.39	1.43 ± 0.31	-1.02 ± 0.24	1.61 ± 0.41	2.03 ± 0.50	1.32 ± 0.36
NM_013538	Cell division cycle associated 3	Cdca3	2.17 ± 0.65	1.45 ± 0.45	1.00 ± 0.28	1.94 ± 0.55	1.96 ± 0.56	1.34 ± 0.41	2.18 ± 0.62	1.78 ± 0.42	1.04 ± 0.26	1.57 ± 0.39	2.03 ± 0.48	1.43 ± 0.39
NM_172301	Cyclin B1	Ccnb1	2.75 ± 0.63	1.66 ± 0.40	1.00 ± 0.30	3.13 ± 0.82	1.85 ± 0.60	1.42 ± 0.43	2.07 ± 0.50	1.62 ± 0.41	1.19 ± 0.29	1.68 ± 0.42	2.09 ± 0.54	1.48 ± 0.51
NM_009831	Cyclin G1	Ccng1	1.30 ± 0.32	1.47 ± 0.49	1.12 ± 0.23	1.53 ± 0.47	1.35 ± 0.36	-1.01 ± 0.27	1.30 ± 0.34	1.55 ± 0.33	1.25 ± 0.34	1.36 ± 0.31	1.52 ± 0.39	1.31 ± 0.29
NM_031166	Inhibitor of DNA binding 4	Id4	1.27 ± 0.38	1.65 ± 0.48	1.07 ± 0.28	1.57 ± 0.47	2.20 ± 0.65	1.70 ± 0.59	1.36 ± 0.41	1.89 ± 0.53	1.15 ± 0.34	-1.41 ± 0.21	1.93 ± 0.56	2.11 ± 0.76

			Time-points											
			300μM AMPA			100μM KA			200μM NMDA			250μM Glu		
Genbank	**Gene Title**	**Symbol**	**5h**	**15h**	**24h**	**5h**	**15h**	**24h**	**5h**	**15h**	**24h**	**5h**	**15h**	**24h**
NM_010578	Integrin beta 1 (fibronectin receptor beta)	Itgb1	1.58 ± 0.33	1.29 ± 0.23	1.13 ± 0.22	1.59 ± 0.30	1.64 ± 0.31	1.13 ± 0.23	1.54 ± 0.31	1.45 ± 0.29	1.10 ± 0.20	1.34 ± 0.22	1.64 ± 0.28	1.46 ± 0.32
NM_023317	Nuclear distribution gene E homolog 1 (A nidulans)	Nde1	1.40 ± 0.39	1.74 ± 0.45	1.11 ± 0.27	1.58 ± 0.42	1.89 ± 0.47	1.57 ± 0.45	1.28 ± 0.32	1.56 ± 0.35	1.24 ± 0.30	1.13 ± 0.30	1.77 ± 0.43	1.35 ± 0.35
NM_007595	Calcium/calmodulin-dependent protein kinase II, beta	Camk2b	-1.04 ± 0.16	-1.57 ± 0.13	-1.52 ± 0.11	1.00 ± 0.16	-2.10 ± 0.08	-2.30 ± 0.10	-1.31 ± 0.13	-2.47 ± 0.06	-1.71 ± 0.11	-1.18 ± 0.13	-2.33 ± 0.09	-1.74 ± 0.11
NM_008913	Protein phosphatase 3, catalytic subunit, alpha isoform	Ppp3ca	1.00 ± 0.23	-1.45 ± 0.25	-1.93 ± 0.09	1.41 ± 0.25	-1.74 ± 0.10	-2.12 ± 0.10	-1.00 ± 0.23	-2.14 ± 0.09	-1.82 ± 0.21	1.03 ± 0.20	-1.71 ± 0.11	-1.48 ± 0.12
NM_023396	Reprimo, TP53 dependent G2 arrest mediator candidate	Rprm	-1.30 ± 0.15	-1.44 ± 0.16	-1.52 ± 0.13	-1.40 ± 0.17	-1.80 ± 0.12	-1.80 ± 0.11	-1.15 ± 0.18	-1.80 ± 0.10	-1.60 ± 0.10	1.00 ± 0.18	-2.00 ± 0.09	-1.90 ± 0.11

Table 2. Genes encoding for proteins involved in mitotic cell division in individual excitotoxicity global transcriptomic profiles. Genes were selected on the basis of demonstrating at least ±1.5 fold-change expression in at least one out of three time-points (5h, 15h and 24h) and passed statistical testing of one-way ANOVA, p <0.05 and FDR correction. The genes were classified in the table according to the first time-point where significant regulation above or below 1.5 is detected.

	300µM AMPA	200µM NMDA	100µM KA	250µM Glu
Up-regulation (5h) **Continue …**	• Anillin, actin binding protein • Aurora kinase A • baculoviral IAP repeat-containing 5 • Buninhibited by benzimidazoles 1 homolog, beta (S. cerevisiae) • Cyclin-dependent kinase 1 • cell division cycle 20 homolog (S. cerevisiae) • cell division cycle associated 2 • cell division cycle associated 3 • cell division cycle associated 5 • cyclin D1 • cyclin D2 • DBF4 homolog (S. cerevisiae) • E4F transcription factor 1 • integrin beta 1 (fibronectin receptor beta) • neural precursor cell expressed, developmentally down-regulated gene 9 • non-SMC condensin I complex, subunit H • polo-like kinase 1 (Drosophila) • predicted gene 8416; predicted gene 5593; cyclin B1; similar to cyclin B1; predicted gene 4870 • regulator of chromosome condensation 2; hypothetical protein LOC100047340	• Anillin, actin binding protein • Aurora kinase A • Baculoviral IAP repeat-containing 5 • Budding uninhibited by benzimidazoles 1 homolog, beta (S. cerevisiae) • Cyclin-dependent kinase 1 • Cell division cycle 20 homolog (S. cerevisiae) • Cell division cycle associated 2 • Cell division cycle associated 3 • Cell division cycle associated 5 • Cell division cycle associated 8 • Cyclin B1 • Cyclin-dependent kinase 2 • DBF4 homolog (S. cerevisiae) • Integrin beta 1 (fibronectin receptor beta) • Kinesin family member C1 • MAD2 mitotic arrest deficient-like 1 (yeast) • Microtubule-associated protein, RP/EB family, member 2 • Neural precursor cell expressed, developmentally down-regulated gene 1 • Non-SMC condensin I complex, subunit H • Nucleolar and spindle associated protein 1 • Pituitary tumor-transforming gene 1	• Anillin, actin binding protein • Asp (abnormal spindle)-like, microcephaly associated (Drosophila) • AT hook containing transcription factor 1 • Aurora kinase A • Baculoviral IAP repeat-containing 5 • Budding uninhibited by benzimidazoles 1 homolog, beta (S. cerevisiae) • Cyclin-dependent kinase 1 • Cell division cycle 20 homolog (S. cerevisiae) • Cell division cycle 6 homolog (S. cerevisiae); • Cell division cycle associated 3 • Cell division cycle associated 5 • Coiled-coil domain containing 99 • Cyclin D1 • Cyclin D2 • Cyclin G1 • Cyclin B1 • Cyclin-dependent kinase 2 • DBF4 homolog (S. cerevisiae) • E4F transcription factor 1 • Inhibitor of DNA binding 4 • Integrin beta 1 (fibronectin receptor beta)	• Anillin, actin binding protein • Aurora kinase A • Baculoviral IAP repeat-containing 5 • Cyclin B1 • Cyclin-dependent kinase 1 • Cell division cycle associated 2 • Cell division cycle associated 3 • Cell division cycle associated 5 • Cell division cycle associated 8 • E4F transcription factor 1 • Nucleolar and spindle associated protein 1 • Polo-like kinase 1 (Drosophila) • Pescadillo homolog 1, containing BRCT domain (zebrafish) • SPC24, NDC80 kinetochore complex component, homolog (S. cerevisiae) • SPC25, NDC80 kinetochore complex component, homolog (S. cerevisiae) • Sperm associated antigen 5

	300μM AMPA	200μM NMDA	100μM KA	250μM Glu
Up-regulation (5h)	• SPC25, NDC80 kinetochore complex component, homolog (S. cerevisiae)	• Polo-like kinase 1 (Drosophila) • SPC24, NDC80 kinetochore complex component, homolog (S. cerevisiae) • SPC25, NDC80 kinetochore complex component, homolog (S. cerevisiae) • Sperm associated antigen 5	• Microtubule-associated protein, RP/EB family, member 2 • Neural precursor cell expressed, developmentally down-regulated gene 9 • Non-SMC condensin II complex, subunit G2 • Nuclear distribution gene E homolog 1 (A nidulans) • Nucleolar and spindle associated protein 1 • ribosomal protein S6 • SET domain containing (lysine methyltransferase) 8 • Kinesin family member C1 • MAD2 mitotic arrest deficient-like 1 (yeast) • SPC25, NDC80 kinetochore complex component, homolog (S. cerevisiae) • sperm associated antigen 5	
Down-regulation at 5h	• NIMA (never in mitosis gene a)-related expressed kinase 3	• Calcium/calmodulin-dependent protein kinase II alpha	• CDK5 and Abl enzyme substrate 1 • NIMA (never in mitosis gene a)-related expressed kinase 3 • SAC3 domain containing 1 • tubulin, gamma 1	

	300μM AMPA	200μM NMDA	100μM KA	250μM Glu
Up-regulation at 15h	• Calcium/calmodulin-dependent protein kinase II, delta • Cyclin G1 • Inhibitor of DNA binding 4 • Nuclear distribution gene E homolog 1 (A nidulans) • Nucleolar and spindle associated protein 1	• Cyclin G1 • E2F transcription factor 6 • Inhibitor of DNA binding 4 • MAD2 mitotic arrest deficient-like 2 (yeast) • Nuclear distribution gene E homolog 1 (A nidulans)	• Anaphase promoting complex subunit 1 • Neural precursor cell expressed, developmentally down-regulated gene 1	• Cell division cycle 20 homolog (S. cerevisiae) • Cyclin G1 • E2F transcription factor 6 • Inhibitor of DNA binding 4 • Integrin beta 1 (fibronectin receptor beta) • Neural precursor cell expressed, developmentally down-regulated gene 1 • Non-SMC condensin I complex, subunit H • Nuclear distribution gene E homolog 1 (A nidulans) • Nuclear factor of activated T-cells, cytoplasmic, calcineurin-dependent 1 • Pituitary tumor-transforming gene 1
Down-regulation at 15h	• Calcium/calmodulin-dependent protein kinase II, beta • Tubulin, beta 3	• Calcium/calmodulin-dependent protein kinase II, beta • Cyclin D1 • Fibronectin type 3 and SPRY domain-containing protein • Protein phosphatase 3, catalytic subunit, alpha isoform • Ras homolog gene family, member U • Stathmin 1 • Tubulin, beta 3	• Budding uninhibited by benzimidazoles 3 homolog (S. cerevisiae) • Calcium/calmodulin-dependent protein kinase II alpha • Calcium/calmodulin-dependent protein kinase II, beta • Protein phosphatase 3, catalytic subunit, alpha isoform • Ras homolog gene family, member U • Regulator of chromosome condensation 2; hypothetical protein LOC100047340 • Calcium/calmodulin-dependent protein kinase II gamma gamma • Stathmin 1	• Amyloid beta (A4) precursor protein • Calcium/calmodulin-dependent protein kinase II alpha • Calcium/calmodulin-dependent protein kinase II, beta • Microtubule-associated protein, RP/EB family, member 2 • Polo-like kinase 2 (Drosophila) • Protein phosphatase 3, catalytic subunit, alpha isoform • Ras homolog gene family, member U

	300μM AMPA	200μM NMDA	100μM KA	250μM Glu
Down-regulation at 24h	• Centrin 2 • Protein phosphatase 3, catalytic subunit, alpha isoform	• Tubulin, gamma 1	• ADP-ribosylation factor-like 8A • Activating transcription factor 6 beta • Centrin 2 • Centrin 3 • Checkpoint with forkhead and ring finger domains • Chromatin modifying protein 1A; predicted gene 8515 • Thioredoxin-like 4B • Tubulin, beta 3	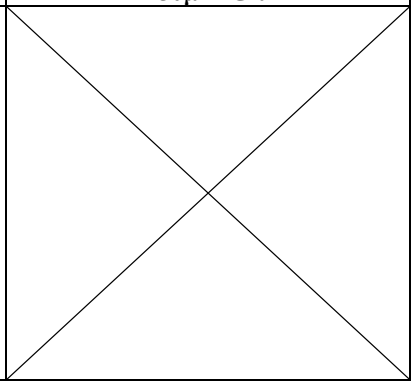

Table 3. Validation of microarray data using real-time PCR technique on mouse culture treated with 250 μM Glu**.** All fold-change expressions are statistically significant at $p < 0.05$. Data are expressed as mean ± sem.

GenBank	Gene Title	Symbol	5h		15h		24h	
			Microarray	Real-time PCR	Microarray	Real-time PCR	Microarray	Real-time PCR
NM_030704	Heat shock protein 8	Hspb8	1.29 ± 0.31	1.42 ± 0.69	4.40 ± 1.06	9.29 ± 0.55	2.63 ± 0.70	2.24 ± 0.72
NM_010442	Heme oxygenase 1	Hmox1	1.59 ± 0.34		2.37 ± 0.41	1.78 ± 0.62	1.51 ± 0.38	
NM_029688	Sulfiredoxin 1 homolog	Srxn1	-1.20 ± 0.29		2.16 ± 0.73	2.99 ± 0.55	1.17 ± 0.43	
NM_011121	Polo-like kinase 1	Plk1	2.08 ± 0.32		2.06 ± 0.37	1.64 ± 0.59	1.62 ± 0.30	
NM_007585	Annexin A2	AnxA2	1.52 ± 0.25		1.93 ± 0.31		2.05 ± 0.43	8.25 ± 0.61
NM_020581	Angiopoietin-like 4	Angptl4	2.00 ± 0.46	3.28 ± 0.66	8.27 ± 1.62		8.24 ± 1.58	5.63 ± 0.58
NM_011497	Aurora kinase A	Aurka	1.91 ± 0.42	3.31 ± 0.69	1.98 ± 0.50	1.95 ± 0.72	1.59 ± 0.44	2.97 ± 1.11
NM_028109	TPX2, microtubule-associated protein homolog	Tpx2	1.70 ± 0.42		2.09 ± 0.55	4.79 ± 0.78	1.57 ± 0.46	4.21 ± 0.60

10. Supplementary data

Supplementary table 1. Significantly expressed genes (with fold-change of at least ±1.5 in a minimum one out of three time-points and passed One-way ANOVA, $p<0.05$) encoding for proteins involved in mitotic cell cycle upon 300µM AMPA-mediated excitotoxicity in cultured primary cortical neurons. Data are expressed as mean ± sem.

			300µM AMPA		
Genbank	**Title**	**Symbol**	**5h**	**15h**	**24h**
Mitotic cell cycle					
NM_172301	Cyclin B1	Ccnb1	2.75 ± 0.63	1.66 ± 0.40	1.03 ± 0.30
NM_007659	Cyclin-dependent kinase 1	Cdk1	2.58 ± 0.62	1.54 ± 0.45	-1.10 ± 0.26
NM_011121	Polo-like kinase 1 (Drosophila)	Plk1	2.40 ± 0.52	1.19 ± 0.42	-1.08 ± 0.20
NM_013726	DBF4 homolog (S. cerevisiae)	Dbf4	2.32 ± 0.55	1.76 ± 0.45	1.25 ± 0.35
NM_011497	Aurora kinase A	AurkA	2.31 ± 0.56	1.48 ± 0.36	1.04 ± 0.25
NM_009829	Cyclin D2	Ccnd2	2.22 ± 0.61	1.50 ± 0.33	1.01 ± 0.18
NM_013538	Cell division cycle associated 3	Cdca3	2.17 ± 0.65	1.45 ± 0.45	1.01 ± 0.28
NM_009773	Budding uninhibited by benzimidazoles 1 homolog, beta (S. cerevisiae)	Bub1b	2.15 ± 0.62	1.34 ± 0.54	-1.09 ± 0.26
NM_028390	Anillin, actin binding protein	Anln	1.97 ± 0.51	1.28 ± 0.28	-1.10 ± 0.19
NM_009689	Baculoviral IAP repeat-containing 5	Birc5	1.94 ± 0.50	1.25 ± 0.37	-1.03 ± 0.26
NM_175384	Cell division cycle associated 2	Cdca2	1.92 ± 0.42	1.12 ± 0.29	-1.12 ± 0.19
NM_173867	Regulator of chromosome condensation 2	Rcc2	1.90 ± 0.59	1.92 ± 0.55	1.64 ± 0.47
NM_026410	Cell division cycle associated 5	Cdca5	1.86 ± 0.38	1.10 ± 0.32	-1.21 ± 0.22
NM_144818	Non-SMC condensin I complex, subunit H	Ncaph	1.83 ± 0.69	1.32 ± 0.63	1.02 ± 0.46
NM_025565	SPC25, NDC80 kinetochore complex component, homolog (S. cerevisiae)	Spc25	1.79 ± 0.52	1.50 ± 0.52	-1.08 ± 0.32
NM_017464	Neural precursor cell expressed, developmentally down-regulated gene 9	Nedd9	1.72 ± 0.47	1.97 ± 0.56	1.31 ± 0.36
NM_023223	Cell division cycle 20 homolog (S. cerevisiae)	Cdc20	1.65 ± 0.52	1.14 ± 0.34	1.03 ± 0.33
NM_010578	Integrin beta 1 (fibronectin receptor beta)	Itgb1	1.58 ± 0.33	1.29 ± 0.23	1.13 ± 0.22
NM_007893	E4F transcription factor 1	E4f1	1.53 ± 0.45	1.42 ± 0.41	1.28 ± 0.38
NM_007631	Cyclin D1	Ccnd1	1.46 ± 0.45	-1.00 ± 0.25	-1.63 ± 0.18

NM_023317	Nuclear distribution gene E homolog 1 (A nidulans)	Nde1	1.40 ± 0.39	1.74 ± 0.45	1.11 ± 0.27
NM_009831	Cyclin G1	Ccng1	1.28 ± 0.32	1.58 ± 0.49	1.05 ± 0.23
NM_023813	Calcium/calmodulin-dependent protein kinase II, delta	Camk2d	1.28 ± 0.38	1.57 ± 0.41	1.24 ± 0.29
NM_031166	Inhibitor of DNA binding 4	Id4	1.27 ± 0.38	1.65 ± 0.48	1.07 ± 0.28
NM_008913	Protein phosphatase 3, catalytic subunit, alpha isoform	Ppp3ca	1.01 ± 0.23	-1.45 ± 0.25	-1.93 ± 0.09
NM_007595	Calcium/calmodulin-dependent protein kinase II, beta	Camk2b	-1.04 ± 0.16	-1.56 ± 0.13	-1.52 ± 0.11
NM_019405	Centrin 2	Cetn2	-1.07 ± 0.24	-1.33 ± 0.24	-1.83 ± 0.21
NM_023279	Tubulin, beta 3 class III	Tubb3	-1.39 ± 0.23	-1.82 ± 0.18	-1.75 ± 0.19
NM_011848	NIMA (never in mitosis gene a)-related expressed kinase 3	Nek3	-1.78 ± 0.13	-1.12 ± 0.16	-1.30 ± 0.13

Supplementary table 2. Significantly expressed genes (with fold-change of at least ±1.5 in a minimum one out of three time-points and passed One-way ANOVA, $p<0.05$) encoding for proteins involved in mitotic cell cycle upon 100µM KA-mediated excitotoxicity in cultured primary cortical neurons. Data are expressed as mean ± sem.

			100µM KA		
Genbank	**Gene title**	**Symbol**	**5h**	**15h**	**24h**
Mitotic cell cycle					
NM_172301	Cyclin B1	Ccnb1	3.13 ± 0.75	1.85 ± 0.39	1.42 ± 0.37
NM_007659	Cyclin-dependent kinase 1	Cdk1	3.02 ± 0.71	1.74 ± 0.38	1.18 ± 0.32
NM_013726	DBF4 homolog (S. cerevisiae)	Dbf4	2.63 ± 0.59	1.76 ± 0.41	1.36 ± 0.32
NM_025565	SPC25, NDC80 kinetochore complex component, homolog (S. cerevisiae)	Spc25	2.38 ± 0.81	1.83 ± 0.57	1.34 ± 0.45
NM_009773	Budding uninhibited by benzimidazoles 1 homolog, beta (S. cerevisiae)	Bub1b	2.33 ± 0.58	1.67 ± 0.50	1.27 ± 0.51
NM_017464	Neural precursor cell expressed, developmentally down-regulated gene 9	Nedd9	2.31 ± 0.74	1.58 ± 0.48	1.38 ± 0.36
NM_011497	Aurora kinase A	AurkA	2.30 ± 0.55	1.46 ± 0.37	1.07 ± 0.29
NM_023223	Cell division cycle 20 homolog (S. cerevisiae)	Cdc20	1.51 ± 0.55	1.35 ± 0.50	1.04 ± 0.46
NM_009829	Cyclin D2	Ccnd2	2.18 ± 0.33	1.26 ± 0.25	1.01 ± 0.34
NM_009689	Baculoviral IAP repeat-containing 5	Birc5	2.09 ± 0.59	1.39 ± 0.35	1.21 ± 0.31
NM_028390	Anillin, actin binding protein	Anln	1.96 ± 0.48	1.60 ± 0.35	1.19 ± 0.32
NM_009791	Asp (abnormal spindle)-like, microcephaly associated (Drosophila)	Aspm	1.95 ± 0.61	1.39 ± 0.45	1.22 ± 0.49
NM_013538	Cell division cycle associated 3	Cdca3	1.94 ± 0.55	1.96 ± 0.56	1.34 ± 0.41
NM_173867	Regulator of chromosome condensation 2	Rcc2	1.88 ± 0.64	2.00 ± 0.56	1.97 ± 0.51
NM_053173	Kinesin family member C1	Kifc5a	1.88 ± 0.50	1.41 ± 0.38	1.17 ± 0.34
NM_007893	E4F transcription factor 1	E4f1	1.84 ± 0.46	1.83 ± 0.47	1.91 ± 0.51
NM_026410	Cell division cycle associated 5	Cdca5	1.82 ± 0.34	1.20 ± 0.30	-1.03 ± 0.23
NM_009096	Ribosomal protein S6	Rps6	1.75 ± 0.45	1.29 ± 0.41	1.23 ± 0.47
NM_133762	Non-SMC condensin II complex, subunit G2	Ncapg2	1.66 ± 0.45	1.17 ± 0.41	-1.03 ± 0.34
NM_010578	Integrin beta 1 (fibronectin receptor beta)	Itgb1	1.59 ± 0.30	1.64 ± 0.31	1.13 ± 0.23
NM_023317	Nuclear distribution gene E homolog 1 (A nidulans)	Nde1	1.58 ± 0.42	1.89 ± 0.47	1.57 ± 0.45
NM_019499	MAD2 mitotic arrest deficient-like 1 (yeast)	Mad2l1	1.58 ± 0.58	1.15 ± 0.41	-1.13 ± 0.40
NM_017407	Sperm associated antigen 5	Spag5	1.57 ± 0.49	1.63 ± 0.39	1.10 ± 0.28
NM_031166	Inhibitor of DNA binding 4	Id4	1.57 ± 0.47	2.19 ± 0.65	1.72 ± 0.59
NM_016756	Cyclin-dependent kinase 2	Cdk2	1.55 ± 0.39	1.31 ± 0.29	1.16 ± 0.30

NM_026375	AT hook containing transcription factor 1	Ahctf1	1.55 ± 0.38	1.27 ± 0.29	1.07 ± 0.29
NM_027411	Coiled-coil domain containing 99	Ccdc99	1.54 ± 0.52	1.10 ± 0.29	1.07 ± 0.38
NM_011799	Cell division cycle 6 homolog (S. cerevisiae)	Cdc6	1.53 ± 0.42	1.06 ± 0.27	1.10 ± 0.34
NM_009831	Cyclin G1	Ccng1	1.53 ± 0.33	1.35 ± 0.25	-1.01 ± 0.22
NM_007631	Cyclin D1	Ccnd1	1.51 ± 0.42	1.06 ± 0.31	-1.28 ± 0.24
NM_030241	SET domain containing (lysine methyltransferase) 8	Setd8	1.51 ± 0.43	-1.07 ± 0.25	-1.14 ± 0.24
NM_153058	Microtubule-associated protein, RP/EB family, member 2	Mapre2	1.50 ± 0.49	1.44 ± 0.42	1.08 ± 0.39
NM_008682	Neural precursor cell expressed, developmentally down-regulated gene 1	Nedd1	1.43 ± 0.33	1.67 ± 0.33	1.23 ± 0.34
NM_008913	Protein phosphatase 3, catalytic subunit, alpha isoform	Ppp3ca	1.41 ± 0.25	-1.74 ± 0.10	-2.12 ± 0.10
NM_019641	Stathmin 1	Stmn1	1.40 ± 0.39	-2.29 ± 0.13	-1.60 ± 0.27
NM_019405	Centrin 2	Cetn2	1.36 ± 0.39	-1.41 ± 0.23	-1.91 ± 0.17
NM_009774	Budding uninhibited by benzimidazoles 3 homolog (S. cerevisiae)	Bub3	1.17 ± 0.31	-1.59 ± 0.14	-1.66 ± 0.16
NM_007684	Centrin 3	Cetn3	1.16 ± 0.32	-1.25 ± 0.19	-1.61 ± 0.19
NM_008569	Anaphase promoting complex subunit 1	Apc1	1.16 ± 0.25	1.61 ± 0.39	1.31 ± 0.35
NM_026823	ADP-ribosylation factor-like 8A	Arl8a	1.15 ± 0.23	-1.37 ± 0.18	-1.78 ± 0.14
NM_145606	Chromatin modifying protein 1A	Chmp1a	1.11 ± 0.26	-1.43 ± 0.13	-1.59 ± 0.12
NM_178597	Calcium/calmodulin-dependent protein kinase type II gamma chain	Camkg	1.10 ± 0.24	-1.69 ± 0.12	-1.71 ± 0.17
NM_007595	Calcium/calmodulin-dependent protein kinase II, beta	Camk2b	1.01 ± 0.16	-2.09 ± 0.08	-2.25 ± 0.10
NM_017406	Activating transcription factor 6 beta	Atf6b	-1.01 ± 0.21	-1.38 ± 0.14	-1.76 ± 0.14
NM_023279	Tubulin, beta 3 class III	Tubb3	-1.13 ± 0.33	-2.22 ± 0.15	-2.58 ± 0.13
NM_177407	Calcium/calmodulin-dependent protein kinase II alpha	Camk2a	-1.15 ± 0.31	-1.62 ± 0.20	-1.54 ± 0.20
NM_172717	Checkpoint with forkhead and ring finger domains	Chfr	-1.16 ± 0.30	-1.42 ± 0.25	-1.67 ± 0.22
NM_133955	Ras homolog gene family, member U	Rhou	-1.32 ± 0.16	-1.98 ± 0.10	-2.18 ± 0.09
NM_175646	Thioredoxin-like 4B	Txnl4b	-1.41 ± 0.21	-1.29 ± 0.20	-1.68 ± 0.16
NM_022021	CDK5 and Abl enzyme substrate 1	Cables1	-1.56 ± 0.14	-1.87 ± 0.12	-2.11 ± 0.12
NM_133678	SAC3 domain containing 1	Sac3d1	-1.58 ± 0.26	-1.55 ± 0.23	-1.80 ± 0.17
NM_134024	Tubulin, gamma 1	Tubg	-1.66 ± 0.13	-1.52 ± 0.13	-1.70 ± 0.15

NM_011848	NIMA (never in mitosis gene a)-related expressed kinase 3	Nek3	-1.79 ± 0.14	-1.20 ± 0.17	-1.68 ± 0.13

Supplementary table 3. Significantly expressed genes (with fold-change of at least ±1.5 in a minimum one out of three time-points and passed One-way ANOVA, $p<0.05$) encoding for proteins involved in mitotic cell cycle upon 200μM NMDA-mediated excitotoxicity in cultured primary cortical neurons. Data are expressed as mean ± sem.

			200μM NMDA		
Genbank	**Genbank**	**Symbol**	**5h**	**15h**	**24h**
Mitotic cell cycle					
NM_013538	Cell division cycle associated 3	Cdca3	2.18 ± 0.62	1.78 ± 0.42	1.04 ± 0.26
NM_025565	SPC25, NDC80 kinetochore complex component, homolog (S. cerevisiae)	Spc25	2.11 ± 0.48	1.82 ± 0.49	1.21 ± 0.32
NM_007659	Cyclin-dependent kinase 1	Cdk1	2.10 ± 0.51	1.66 ± 0.39	1.20 ± 0.26
NM_172301	Cyclin B1	Ccnb1	2.07 ± 0.50	1.62 ± 0.41	1.19 ± 0.29
NM_009689	Baculoviral IAP repeat-containing 5	Birc5	1.96 ± 0.56	1.41 ± 0.33	-1.02 ± 0.22
NM_011121	Polo-like kinase 1 (Drosophila)	Plk1	1.90 ± 0.38	1.44 ± 0.21	-1.10 ± 0.20
NM_019499	MAD2 mitotic arrest deficient-like 1 (yeast)	Mad2l1	1.87 ± 0.62	1.09 ± 0.34	-1.12 ± 0.25
NM_023223	Cell division cycle 20 homolog (S. cerevisiae)	Cdc20	1.87 ± 0.39	1.43 ± 0.31	-1.02 ± 0.24
NM_026410	Cell division cycle associated 5	Cdca5	1.85 ± 0.44	1.26 ± 0.22	-1.11 ± 0.20
NM_144818	Non-SMC condensin I complex, subunit H	Ncaph	1.85 ± 0.64	1.28 ± 0.45	1.10 ± 0.34
NM_028390	Anillin, actin binding protein	Anln	1.84 ± 0.41	1.50 ± 0.33	1.18 ± 0.26
NM_008682	Neural precursor cell expressed, developmentally down-regulated gene 1	Nedd1	1.71 ± 0.42	1.85 ± 0.40	1.36 ± 0.27
NM_011497	Aurora kinase A	AurkA	1.65 ± 0.40	1.31 ± 0.32	1.11 ± 0.26
NM_016756	Cyclin-dependent kinase 2	Cdk2	1.60 ± 0.28	1.48 ± 0.26	1.33 ± 0.29
NM_009773	Budding uninhibited by benzimidazoles 1 homolog, beta (S. cerevisiae)	Bub1b	1.60 ± 0.41	1.28 ± 0.39	-1.06 ± 0.26
NM_053173	Kinesin family member C1	Kifc5a	1.59 ± 0.44	1.19 ± 0.26	1.01 ± 0.21
NM_026560	Cell division cycle associated 8	Cdca8	1.58 ± 0.48	1.22 ± 0.32	1.01 ± 0.27
NM_175384	Cell division cycle associated 2	Cdca2	1.57 ± 0.30	1.32 ± 0.25	-1.01 ± 0.20
NM_013917	Pituitary tumor-transforming gene 1	Pttg1	1.57 ± 0.62	1.09 ± 0.29	-1.23 ± 0.21
NM_026282	SPC24, NDC80 kinetochore complex component, homolog (S. cerevisiae)	Spc24	1.55 ± 0.50	1.29 ± 0.37	-1.06 ± 0.25
NM_017407	Sperm associated antigen 5	Spag5	1.54 ± 0.37	1.43 ± 0.32	1.02 ± 0.22
NM_010578	Integrin beta 1 (fibronectin receptor beta)	Itgb1	1.54 ± 0.31	1.45 ± 0.29	1.10 ± 0.20
NM_013726	DBF4 homolog (S. cerevisiae)	Dbf4	1.51 ± 0.40	1.11 ± 0.23	1.28 ± 0.35
NM_033270	E2F transcription factor 6	E2f6	1.41 ± 0.32	1.50 ± 0.24	1.15 ± 0.23

NM_031166	Inhibitor of DNA binding 4	Id4	1.36 ± 0.41	1.89 ± 0.53	1.15 ± 0.34
NM_027985	MAD2 mitotic arrest deficient-like 2 (yeast)	Mad2l2	1.33 ± 0.29	1.50 ± 0.37	1.05 ± 0.27
NM_009831	Cyclin G1	Ccng1	1.30 ± 0.34	1.55 ± 0.33	1.25 ± 0.34
NM_023317	Nuclear distribution gene E homolog 1 (A nidulans)	Nde1	1.28 ± 0.32	1.56 ± 0.35	1.24 ± 0.30
NM_019641	Stathmin 1	Stmn1	1.19 ± 0.39	-1.80 ± 0.16	-1.34 ± 0.22
NM_023279	Tubulin, beta 3 class III	Tubb3	1.02 ± 0.31	-1.77 ± 0.17	-1.66 ± 0.17
NM_007631	Cyclin D1	Ccnd1	1.02 ± 0.31	-1.61 ± 0.15	-1.65 ± 0.15
NM_008913	Potein phosphatase 3, catalytic subunit, alpha isoform	Ppp3ca	-1.00 ± 0.23	-2.14 ± 0.09	-1.82 ± 0.21
NM_134024	Tubulin, gamma 1	Tubg1	-1.04 ± 0.18	-1.34 ± 0.15	-1.76 ± 0.13
NM_153058	Microtubule-associated protein, RP/EB family, member 2	Mapre2	-1.29 ± 0.16	-1.63 ± 0.11	-1.27 ± 0.25
NM_183178	Fibronectin type 3 and SPRY domain-containing protein	Fsd1	-1.30 ± 0.15	-1.72 ± 0.12	-1.69 ± 0.11
NM_007595	Calcium/calmodulin-dependent protein kinase II, beta	Camk2b	-1.31 ± 0.13	-2.47 ± 0.06	-1.71 ± 0.11
NM_133955	Ras homolog gene family, member U	Rhou	-1.53 ± 0.14	-1.50 ± 0.12	-1.22 ± 0.20
NM_177407	Calcium/calmodulin-dependent protein kinase II alpha	Camk2a	-1.62 ± 0.18	-1.68 ± 0.16	-1.43 ± 0.17

Supplementary table 4. Significantly expressed genes (with fold-change of at least ±1.5 in a minimum one out of three time-points and passed One-way ANOVA, $p<0.05$) encoding for proteins involved in mitotic cell cycle upon 250µM Glu-mediated excitotoxicity in cultured primary cortical neurons. Data are expressed as mean ± sem.

			250µM Glu		
Genbank	**Gene**	**Symbol**	**5h**	**15h**	**24h**
Mitotic cell cycle					
NM_011121	Polo-like kinase 1 (Drosophila)	Plk1	2.08 ± 0.32	2.06 ± 0.37	1.62 ± 0.30
NM_007659	Cyclin-dependent kinase 1	Cdk1	2.06 ± 0.42	1.91 ± 0.47	1.50 ± 0.39
NM_011497	Aurora kinase A	AurkA	1.91 ± 0.42	1.98 ± 0.50	1.59 ± 0.44
NM_026410	Cell division cycle associated 5	Cdca5	1.88 ± 0.45	1.60 ± 0.35	1.35 ± 0.33
NM_175384	Cell division cycle associated 2	Cdca2	1.82 ± 0.37	1.70 ± 0.35	1.52 ± 0.34
NM_028390	Anillin, actin binding protein	Anln	1.80 ± 0.40	1.86 ± 0.51	1.67 ± 0.41
NM_026282	SPC24, NDC80 kinetochore complex component, homolog (S. cerevisiae)	Spc24	1.71 ± 0.32	1.67 ± 0.55	1.18 ± 0.33
NM_172301	Cyclin B1	Ccnb1	1.68 ± 0.42	2.09 ± 0.54	1.48 ± 0.51
NM_025565	SPC25, NDC80 kinetochore complex component, homolog (S. cerevisiae)	Spc25	1.66 ± 0.41	1.85 ± 0.65	1.47 ± 0.63
NM_023223	Cell division cycle 20 homolog (S. cerevisiae)	Cdc20	1.61 ± 0.41	2.03 ± 0.50	1.32 ± 0.36
NM_026560	Cell division cycle associated 8	Cdca8	1.61 ± 0.57	1.43 ± 0.48	1.06 ± 0.36
NM_013538	Cell division cycle associated 3	Cdca3	1.57 ± 0.39	2.03 ± 0.48	1.43 ± 0.39
NM_009689	Baculoviral IAP repeat-containing 5	Birc5	1.54 ± 0.36	1.88 ± 0.50	1.34 ± 0.30
NM_017407	Sperm associated antigen 5	Spag5	1.52 ± 0.38	1.85 ± 0.46	1.55 ± 0.48
NM_007893	E4F transcription factor 1	E4f1	1.52 ± 0.40	1.09 ± 0.33	1.03 ± 0.35
NM_008682	Neural precursor cell expressed, developmentally down-regulated gene 1	Nedd1	1.40 ± 0.29	1.84 ± 0.42	1.65 ± 0.42
NM_009831	Cyclin G1	Ccng	1.36 ± 0.31	1.52 ± 0.39	1.31 ± 0.29
NM_010578	Integrin beta 1 (fibronectin receptor beta)	Itgb1	1.34 ± 0.22	1.64 ± 0.28	1.46 ± 0.32
NM_013917	Pituitary tumor-transforming gene 1	Pttg1	1.29 ± 0.44	1.71 ± 0.72	1.27 ± 0.45
NM_144818	Non-SMC condensin I complex, subunit H	Ncaph	1.24 ± 0.49	1.71 ± 0.55	1.53 ± 0.49
NM_033270	E2F transcription factor 6	E2f6	1.22 ± 0.24	1.68 ± 0.42	1.53 ± 0.39
NM_023317	Nuclear distribution gene E homolog 1 (A nidulans)	Nde1	1.13 ± 0.30	1.77 ± 0.43	1.35 ± 0.35
NM_022889	Pescadillo homolog 1, containing BRCT domain (zebrafish)	Pes1	1.12 ± 0.22	1.49 ± 0.33	1.31 ± 0.28
NM_007471	Amyloid beta (A4) precursor protein	App	1.06 ± 0.20	-1.64 ± 0.12	-1.56 ± 0.14
NM_008913	Protein phosphatase 3, catalytic subunit, alpha isoform	Ppp3ca	1.03 ± 0.20	-1.71 ± 0.11	-1.48 ± 0.12

NM_007595	Calcium/calmodulin-dependent protein kinase II, beta	Camk2b	-1.18 ± 0.13	-2.33 ± 0.09	-1.74 ± 0.11
NM_198429	Nuclear factor of activated T-cells, cytoplasmic, calcineurin-dependent 1	Nfatc1	-1.29 ± 0.23	1.50 ± 0.41	1.61 ± 0.45
NM_153058	Microtubule-associated protein, RP/EB family, member 2	Mapre2	-1.29 ± 0.15	-1.51 ± 0.14	-1.27 ± 0.17
NM_133955	Ras homolog gene family, member U	Rhou	-1.30 ± 0.16	-1.62 ± 0.15	-1.31 ± 0.14
NM_152804	Polo-like kinase 2 (Drosophila)	Plk2	-1.37 ± 0.18	-1.82 ± 0.12	-1.46 ± 0.20
NM_031166	Inhibitor of DNA binding 4	Id4	-1.41 ± 0.21	1.93 ± 0.56	2.11 ± 0.76
NM_177407	Calcium/calmodulin-dependent protein kinase II alpha	Camk2a	-1.42 ± 0.19	-1.67 ± 0.21	-1.44 ± 0.24